IEEE Access
Multidisciplinary | Rapid Review | Open Access Journal

Received July 9, 2020, accepted August 2, 2020, date of publication August 6, 2020, date of current version August 24, 2020.

Digital Object Identifier 10.1109/ACCESS.2020.3014719

Rear-Wheel Steering Control for Enhanced Steady-State and Transient Vehicle Handling Characteristics

KWANWOO PARK[1], EUNHYEK JOA[2], KYONGSU YI[1], (Member, IEEE), AND YOUNGSIK YOON[3]

[1]Department of Mechanical and Aerospace Engineering, Seoul National University, Seoul 08826, South Korea
[2]Department of Mechanical Engineering, University of California at Berkeley, Berkeley, CA 94701, USA
[3]Hyundai Motor Company R&D Center, Hwaseong 18280, South Korea

Corresponding author: Kyongsu Yi (kyi@snu.ac.kr)

This work was supported by the National Research Foundation of Korea (NRF) Grant funded by the Ministry of Science, Information & Communication Technology (ICT), and Future Planning (MSIP) under Grant NRF-2016R1E1A1A01943543.

ABSTRACT This paper presents a rear-wheel steering (RWS) control algorithm to enhance the vehicle handling performance without prior knowledge of tire characteristics. A RWS system is a chassis control module that can effectively improve vehicle maneuverability and stability. Since the tire-road friction coefficient is difficult to obtain in real world application, the proposed RWS control algorithm is designed so that it can be implemented without any tire-road information. The proposed RWS control algorithm consists of steady-state and transient control inputs. The steady-state control input is proportional to the driver's steering input for achieving the desired yaw rate gain. The desired yaw rate gain is obtained through an offline optimization that is aimed to minimize the vehicle lateral velocity. The transient control input consists of feedforward and feedback control inputs. The feedforward input is designed to improve transient responses of the yaw rate. Computer simulation studies have shown that a trade-off relationship between overshoot and response time exists when the RWS control input is a sum of the steady-state and feedforward inputs. To compromise this conflict, a feedback input has been designed. The overshoot can be significantly reduced while the response time is slightly changed via the feedback input. The proposed algorithm has been investigated via computer simulations. The simulation has been conducted for step steer and sine with dwell scenarios under various road friction conditions. The performance of a RWS vehicle was evaluated using objective indices. Simulation results show that the proposed algorithm enhances vehicle handling performance.

INDEX TERMS Rear-wheel steering control, vehicle handling, maneuverability, lateral stability, lateral transient response, performance evaluation.

NOMENCLATURE

α_f/α_r	Front/rear tire slip angle $[rad]$
δ_f/δ_r	Front/rear wheel steer angle $[rad]$
β	Vehicle side slip angle $[rad]$
η	A new design parameter in feedforward of transient control input []
γ	Vehicle yaw rate $[rad/s]$
μ	Road friction []
ω_d	Damped natural frequency of system [Hz]
ω_n	Natural frequency of system [Hz]
τ	Time constant of 1^{st} order delay [s]
ζ	Damping ratio of system []
a_y	Vehicle lateral acceleration $[m/s^2]$
a_{ij}	Element of matrix A at the i-th row and j-th column
b_i/c_i	Element of matrix B/C at the i-th row
C_f/C_r	Front/rear tire cornering stiffness $[N/rad]$
F_{yf}	Lateral force of front tire $[N]$
F_{yr}	Lateral force of rear tire $[N]$
G_{ss}^{γ}	Steady-state yaw rate gain []
I_z	Yaw moment inertia of vehicle $[kg \cdot m^2]$
k_δ	Gain of rear-wheel steering in steady-state [ ]
K_{fb}	Feedback gain []
K_{us}	Understeer gradient $[rad \cdot s^2/m]$
L	Distance from the front axle to the rear axle $[m]$

The associate editor coordinating the review of this manuscript and approving it for publication was Ning Sun.

l_f/l_r	Distance from the center of gravity to the front/rear axle $[m]$
m	Total mass of vehicle $[kg]$
M_z	Yaw moment $[N \cdot m]$
N_r	Steering gear ratio []
R	Radius of curvature [m]
s	Laplace operator
t	Time $[s]$
V_x	Vehicle longitudinal velocity $[m/s]$
V_y	Vehicle lateral velocity $[m/s]$

I. INTRODUCTION

Rear-wheel steering (RWS) control has been developed for decades with the aim of improving vehicle handling performance and stability. Steering the rear wheels offers control of rear lateral tire forces, and RWS systems offer great advantages in urban driving situations and on the highway. In the urban driving situations such as cornering in a narrow alley, the driver's burden to exert steering wheel angle can be reduced when the curvature changes suddenly because the RWS system increases the vehicle's yaw rate gain by steering the rear wheels in the opposite direction to the front wheels. In the highway driving situations, the vehicle's lateral stability can be improved throughout the driving range from mild handling to limit handling maneuvers because the RWS system decreases yaw rate gain by rear wheels in the same direction as the front wheels.

The purposes of RWS control broadly fall into two categories: 1) minimize vehicle side slip angle, and 2) track the desired yaw rate. Early rear-wheel steering control methods have been used to enhance vehicle stability and maneuverability by regulating the side slip angle [1]–[4]. Nagai *et al.* [2] designed a state feedback controller to maintain the zero-side slip angle by constructing the model-following RWS control. Lee *et al.* [3] proposed a control strategy, i.e., 'four-wheel independent steering.' This control strategy aimed to reduce not only the side slip angle but also the actuating power. Eguchi *et al.* [4] considered both vehicle lateral dynamics and suspension dynamics such as roll steer and compliance steer to make the side slip angle equal to zero.

A number of studies have been proposed to enhance the vehicle's stability and maneuverability by tracking the output of the reference vehicle model. Lv *et al.* [5] proposed a yaw rate tracking four-wheel steering (4WS) by means of multi-objective H optimal control. This proposed algorithm accomplishes desired handling characteristics with fewer state variables than conventional model-following control methods. Wagner *et al.* [6] performed and compared the performance of active steering controllers through the optimization. Concretely, Wagner *et al.* evaluated front-wheel steering (FWS), rear-wheel steering (RWS), and all-wheel steering (AWS) for the tracking performance of the desired vehicle yaw rate and lateral speed. They concluded that RWS control shows the best performance in terms of actuator costs and vehicle lateral behavior. However, these model-based methods need to pinpoint parameters between the tire and road surface as well as the vehicle parameters.

Most model-based RWS control methods utilize a model that consists of vehicle lateral dynamics and tire dynamics. Based on such models, the RWS or 4WS control inputs are obtained by assuming that the correct vehicle model and parameters are known. Therefore, the performance of control methods can deteriorate when the uncertainties of the vehicle modeling and parameters are presented. For instance, when the driver negotiates a corner with high lateral acceleration conditions, the tire characteristics enter the nonlinear region. In this case, there are differences between nominal and actual parameters, and such parameter errors deteriorate the algorithm's performance [7]–[10]. Therefore, practitioners often have laborious tasks such as adjusting control gains and parameters. To resolve this inconvenience, there are some methods to design a robust controller in consideration of uncertainties. Russell and Gerdes [11] proposed a state feedback controller to track a reference model and demonstrated stability and robustness to the model uncertainties. Akar [12] proposed a sliding mode controller to track both zero-side slip angle and reference yaw rate, which showed robustness against parameter variations.

In contrast to the model-based control methods that are widely researched, many car manufacturers have adopted a simple proportional RWS control algorithm for application in mass production process. In the proportional RWS control, the proportional gain is the ratio of the rear-wheel steering angle to the front wheel steering angle as a function of vehicle speed. This gain is designed to minimize the steady-state side slip angle. At low speeds, RWS is controlled in the opposite direction (i.e. reverse-phase) to the front wheels for increasing the yaw rate gain while at high speeds RWS is controlled in the same direction (i.e. in-phase) for enhancing the vehicle stability. However, such simple proportional RWS control has some problems via vehicle tests [13]. Bredthauer and Lynch [13] investigated the simple proportional RWS control with respect to various tire types such as winter tires and racing tires. Many test drivers suggest that unpleasant vehicle behavior could occur with respect to quick steering inputs and rear-wheel steering calibrations for tires. This is because the simple proportional RWS control does not consider the vehicle's transient response. There are more advanced control methods that consider the transient response in RWS control input to resolve this unnatural vehicle lateral behavior. Cho and Kim [14] designed a delayed RWS whereby the time delay between the front-wheel and rear-wheel is extracted from the responses of the optimal 4WS control. Nissan's phase reversal control [4] considers the suspension characteristics and demonstrated significantly improved vehicle response at high speeds compared to proportional control and first-order delay control [15], [16]. However, Nissan's control logic requires tire and suspension parameters, and errors can degrade the performance of the control algorithm.

This paper proposes a new RWS control design framework that can modify the vehicle handling characteristics using

measurable vehicle signals, and, more importantly, without any information from the tire. The proposed RWS control law is a sum of steady-state and transient control inputs. The steady-state part of the proposed algorithm is designed to be proportional to the driver's steering wheel angle input. This steady-state input modifies steady-state handling characteristics according to vehicle speeds. At low speeds, RWS is controlled in the opposite direction (reversed-phase) to the front-wheels for increasing the vehicle agility (increase yaw rate gain). At high speeds, RWS is controlled in the same direction (in-phase) to the front-wheels for improved vehicle stability (reduced yaw rate gain). The transient control input adjusts the vehicle's transient response without any information from the tire. To design such transient control input, new vehicle dynamic models and new design parameters are proposed to exclude such tire parameters. Transient responses such as overshoot, rise time, and peak response time are a function of vehicle and tire parameters, and the transient control input can be designed without tire parameters via the proposed control design framework.

The main contributions of the proposed RWS control design framework are as follows:

1) The proposed control algorithm improves vehicle handling performance using measurable sensor signals (such as yaw rate, lateral acceleration, and steering wheel angle) without any information on tire and road surface.
2) This paper proposes a new chassis control design flow: (1) offline optimization; (2) parameterization of optimal solutions; (3) control design.
3) This paper proposes a new lateral dynamic model to design control law.
4) This paper proposes a transient control input without any tire and road friction information based on the proposed lateral dynamic model.

II. LATERAL VEHICLE DYNAMICS OF 4WS VEHICLE

A single-track (bicycle) vehicle model (Figure 1) has been used to describe the vehicle lateral dynamics with RWS control input [7], [17]. The equation of motion can be derived from the bicycle model in Figure 1:

$$\begin{aligned} \Sigma F_y &= F_{yf} + F_{yr} = mV_x\left(\dot{\beta} + \gamma\right) \\ \Sigma M_z &= F_{yf} l_f - F_{yr} l_r = I_z \dot{\gamma} \end{aligned} \tag{1}$$

The state equation is organized with the two vehicle state variables: 1) side slip angle β; and 2) yaw rate γ.

Assuming that linear behavior of lateral tire forces the tire slip angles, the tire forces can be described as:

$$F_{yf} = C_f \cdot \left(\underbrace{\delta_f - \beta - \frac{l_f \gamma}{V_x}}_{\alpha_f} \right)$$

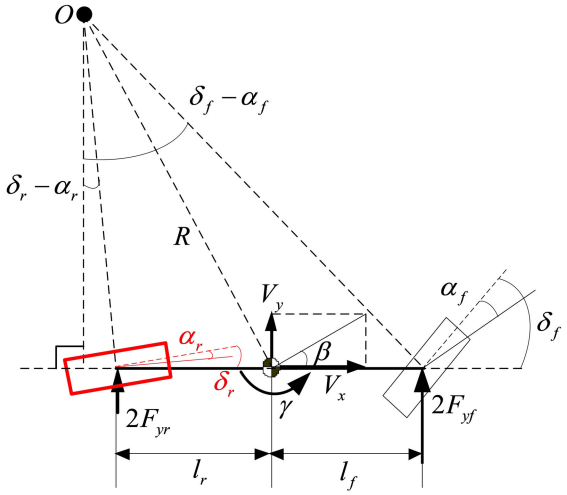

FIGURE 1. A single-track vehicle model for the 4WS vehicle.

$$F_{yr} = C_r \cdot \left(\underbrace{\delta_r - \beta + \frac{l_r \gamma}{V_x}}_{\alpha_r} \right) \tag{2}$$

where α_f and α_r are the slip angles of the front and rear tire, respectively. The tire slip angles are defined by the kinematic relationship with steer angles and vehicle states. The tire lateral forces are actually calculated as $F_{y,(f/r)}(k) = C_{(f/r)}(k) \cdot \alpha_{(f/r)}(k)$, and the tire cornering stiffness C_f and C_r are the nonlinear coefficients that well represent the vehicle lateral behavior at k step.

From (1) and (2), the state equation of the bicycle model with RWS can be written as

$$\begin{aligned} \dot{x}(t) &= A \cdot x(t) + B \cdot \delta_f(t) + C \cdot \delta_r(t) \\ A &= \begin{bmatrix} -\dfrac{(C_f + C_r)}{mV_x} & -\dfrac{(C_f l_f - C_r l_r)}{mV_x^2} - 1 \\ -\dfrac{(C_f l_f - C_r l_r)}{I_z} & -\dfrac{\left(C_f l_f^2 + C_r l_r^2\right)}{I_z V_x} \end{bmatrix}, \\ B &= \begin{bmatrix} \dfrac{C_f}{mV_x} \\ \dfrac{C_f l_f}{I_z} \end{bmatrix}, \quad C = \begin{bmatrix} \dfrac{C_r}{mV_x} \\ -\dfrac{C_r l_r}{I_z} \end{bmatrix} \end{aligned} \tag{3}$$

where, the vehicle state $x(t)$ is $\begin{bmatrix} \beta & \gamma \end{bmatrix}^T$.

At steady-state, the derivative terms in (3) are zero ($\dot{\beta} = 0$, $\dot{\gamma} = 0$), and the vehicle dynamics in (3) shrinks to the vehicle cornering kinematics as follows:

$$\delta_f - \delta_r = \frac{L}{V_x}\gamma_{ss} + \underbrace{\frac{m}{L}\left(\frac{l_r}{C_f} - \frac{l_f}{C_r}\right)}_{K_{us}} \cdot V_x \gamma_{ss} \tag{4}$$

where γ_{ss} is the yaw rate in the steady-state, and K_{us} is the understeer gradient that shows the steering characteristic of the vehicle. The rear-wheel steering angle δ_r affects vehicle cornering kinematics.

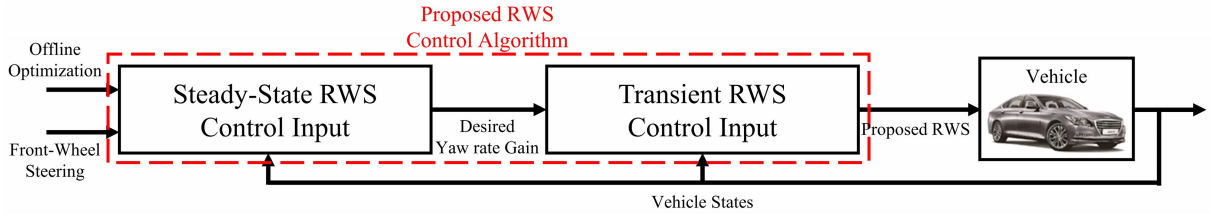

FIGURE 2. Block diagram for proposed rear-wheel steering control.

For conventional vehicles without the rear-wheel steering system ($\delta_r = 0$) case, the cornering kinematics and the steady-state yaw rate gain of FWS vehicle $G^{\gamma}_{ss,FWS}$ are derived as:

$$\delta_f = \left(\frac{L}{V_x} + K_{us}V_x\right) \cdot \gamma_{ss} \tag{5}$$

$$G^{\gamma}_{ss,FWS} = \frac{\gamma_{ss}}{\delta_f} = \frac{V_x}{L + K_{us}V_x^2} \tag{6}$$

For vehicles with the rear wheel system ($\delta_r \neq 0$) case, the steady-state yaw rate gain for the RWS vehicle $G^{\gamma}_{ss,RWS}$ can be written as follows:

$$G^{\gamma}{}_{ss,RWS} = \frac{\gamma_{ss,RWS}}{\delta_f} = \frac{V_x}{L + K_{us} \cdot V_x^2} \cdot \left(1 - \frac{\delta_{r,ss}}{\delta_f}\right)$$
$$= G^{\gamma}{}_{ss,FWS} \cdot \left(1 - \frac{\delta_{r,ss}}{\delta_f}\right) \tag{7}$$

where $\gamma_{ss,RWS}$ is the steady-state yaw rate of RWS vehicle, and $\delta_{r,ss}$ is the rear-wheel steering input in the steady-state. The steady-state yaw rate gain for RWS vehicle is proportional to that for FWS vehicle as described in (6) and (7). Moreover, the ratio between two steady-state gains is a function of front and rear steering wheel angles. Therefore, the steady-state cornering characteristics can be modified by controlling the rear-wheel steering angle proportional to the front-wheel steering angle (the driver's input). The details of modifying the steady-state cornering characteristics are elucidated in the next chapter.

This paper uses values the vehicle parameters from Table 1. These vehicle parameters were tuned to show similar dynamic characteristics of the given test vehicle—an F-segment vehicle with Rear-Wheel Drive (RWD).

TABLE 1. Nominal values of vehicle parameter.

Parameter (Notation)	Value (Units)
Total mass (m)	2055.14 [kg]
Yaw moment inertia (I_z)	4551 [kg · m^2]
Wheel base (L)	3.009 [m]
Distance from C.G to front wheels (l_f)	1.477 [m]
Distance from C.G to rear wheels (l_r)	1.532 [m]
Steering gear ratio (N_r)	15.221
Understeer Gradient (K_{us})	0.0063 [rad · s^2/m]

III. CONTROLLER DESIGN

This section details a new rear-wheel steering (RWS) control algorithm. The proposed algorithm is a combination of the steady-state and transient control inputs as shown in Figure 2.

The steady-state RWS control input is proportional to the driver's front-wheel steering. The proportional gain is obtained through offline numerical optimization. The transient control input improves the transient handling response such as overshoot, rise time, and peak response. The vehicle transient response can be deteriorated with sole steady-state RWS control (the proportional control). For example, the lateral acceleration response of the proportional control is unnatural compared to that of the base vehicle (Figure 3). Figure 3 (a) shows the rear-wheel steering input proportional to the front-wheels, and Figure 3 (b) shows lateral acceleration responses. The base is the FWS vehicle with the specification of Table 1. The RWS is a vehicle with the proportional controller. The computed value is the multiplication of the yaw rate and vehicle speed, which means the steady-state lateral acceleration of the RWS vehicle.

The previous research [13] showed experimentally that this unnatural lateral jerk makes the driver feel unpleasant. This unnatural lateral jerk results from transient handling characteristics—especially the first-time derivative of the side slip angle. There is a difference between the lateral acceleration and the multiplication of the vehicle speed and yaw rate (Figure 3 (b)). Since this difference denotes the first-time derivative of the side slip angle, we conclude that this term is the cause of this unnatural lateral jerk.

To improve this issue, previous studies [14]–[16] added a 1st-order delay term to the rear wheel steering control algorithm. Adding such a delay term improves the lateral transient response by reducing the phase delay between the yaw rate and the lateral acceleration. Here, the previous approach to add a 1st order delay is expanded. The transient RWS control input consists of two parts: (1) feedforward input to control the delay of the yaw rate response, and (2) feedback input to control the first-time derivative of the side slip angle.

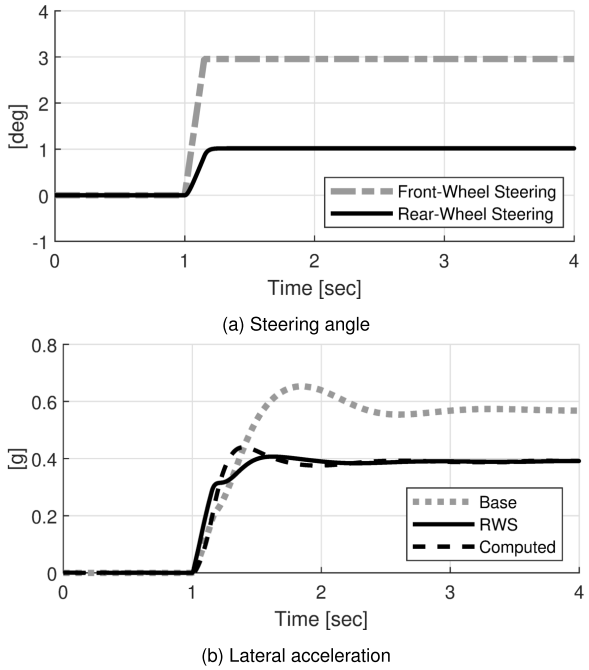

FIGURE 3. A comparison of lateral acceleration of base vehicle and RWS vehicle. 110kph, 45deg(300deg/s) step steer scenario.

In summary, the proposed RWS control algorithm consists of the steady-state input, the feedforward of transient input (w.r.t. delay of the yaw rate) and the feedback of transient input (w.r.t. the first-time derivative of the side slip angle). The most notable point is that the proposed control algorithm only uses vehicle specifications and measurable vehicle signals instead of the tire cornering stiffness in the vehicle dynamics.

A. REAR-WHEEL STEERING CONTROL FOR ENHANCED STEADY-STATE HANDLING

The goal of the steady-state RWS control is to minimize the steady-state side slip angle by modifying the vehicle's steady-state response. It is well-known that this goal can be accomplished with the RWS input that is proportional to the driver's front steering wheel angle [13-16]. Therefore, the steady-state control RWS input in this paper is designed to be proportional to front-wheel steering as follows:

$$\delta_{r,ss}(t) = k_\delta(V_x) \cdot \delta_f(t) \tag{8}$$

where, $\delta_{r,ss}$ is the steady-state control input of the proposed rear-wheel steering, and k_δ is the proportional gain to the front-wheel steering.

The steady-state yaw rate response generated by (8) can be re-written using (7) as follows:

$$\begin{aligned} G^\gamma{}_{ss,RWS} &= G^\gamma{}_{ss,FWS} \cdot \left(1 - \frac{\delta_{r,ss}}{\delta_f}\right) \\ &= G^\gamma{}_{ss,FWS} \cdot (1 - k_\delta) \end{aligned} \tag{9}$$

As described in (9), the steady-state yaw rate gain of RWS vehicles is a multiple of that of the FWS vehicles, and the proportional gain k_δ is a design variable. As this gain increases (or decreases), the steady-state yaw rate gain of RWS vehicles decreases (or increases) relative to that of FWS vehicles.

Designing the proportional gain k_δ is important because the proportional gain k_δ is the sole design variable to modify the steady-state response of vehicles. In this paper, a steady-state gain is designed through offline numerical optimization results. The control objective of the optimization is selected based on [6]. Wagner *et al.* conducted a performance comparison by configuring various active steering controls to track the reference trajectory. The active steering configurations are the passive vehicle (*Base*), single-actuation configurations for reference yaw rate tracking (FWS^γ, RWS^γ), and for lateral velocity minimization (FWS^{V_y}, RWS^{V_y}), and all-wheel steering (*AWS*) for tracking both references. Wagner *et al.* concluded that RWS^{V_y} shows the best performance when comparing the actuator cost and objective assessments with the various criteria. Therefore, in this paper, RWS^{V_y} control based on the optimization plant in [6] has been adopted for the offline numerical optimization.

The optimization results are presented in Figure 4. Figure 4 (a) represents the ratio of RWS yaw rate gain to FWS gain ($G^\gamma_{ss,RWS}/G^\gamma_{ss,FWS}$), and (b) shows the proportional gain (k_δ) of steady-state control input. The proportional gain becomes smaller than zero at low speeds to increase the yaw rate gain; as a result, steady-state RWS input is controlled in the reverse-phase as the front-wheel steering. Conversely, the steady-state RWS input at high speeds reduces the yaw rate gain to improve vehicle stability by steering in the in-phase as the front-wheels. Correspondingly, the proportional gain is bigger than zero, and the control input is set to in-phase to the front-wheel steering. The speed is about 56kph when the steady-state RWS gain is zero. The results are consistent with how practitioners design the RWS control. Typically, RWS is controlled in the reverse-phase to enhance the yaw rate response at low speed while it is controlled in the in-phase to enhance the vehicle stability at high speeds.

In conclusion, the proportional gain k_δ from the optimization results and the steady-state control input $\delta_{r,ss}$ of (8) are re-arranged using the yaw rate gains of (9):

$$k_\delta(V_x) = 1 - \frac{G^\gamma_{ss,RWS}}{G^\gamma_{ss,FWS}}(V_x) \tag{10}$$

$$\begin{aligned} \delta_{r,ss}(t) &= k_\delta(V_x) \cdot \delta_f(t) \\ &= \left(1 - \frac{G^\gamma_{ss,RWS}}{G^\gamma_{ss,FWS}}(V_x)\right) \cdot \delta_f(t) \end{aligned} \tag{11}$$

However, the control input in (10) and (11) results in an unnatural lateral jerk as illustrated in Figure 3. Therefore, in this paper, the transient control input is designed to compensate for the unnatural lateral jerk.

B. REAR-WHEEL STEERING CONTROL FOR ENHANCED TRANSIENT HANDLING – FEEDFORWARD CONTROLLER

The transient RWS control input consists of model-based feedforward and feedback parts. In this subsection,

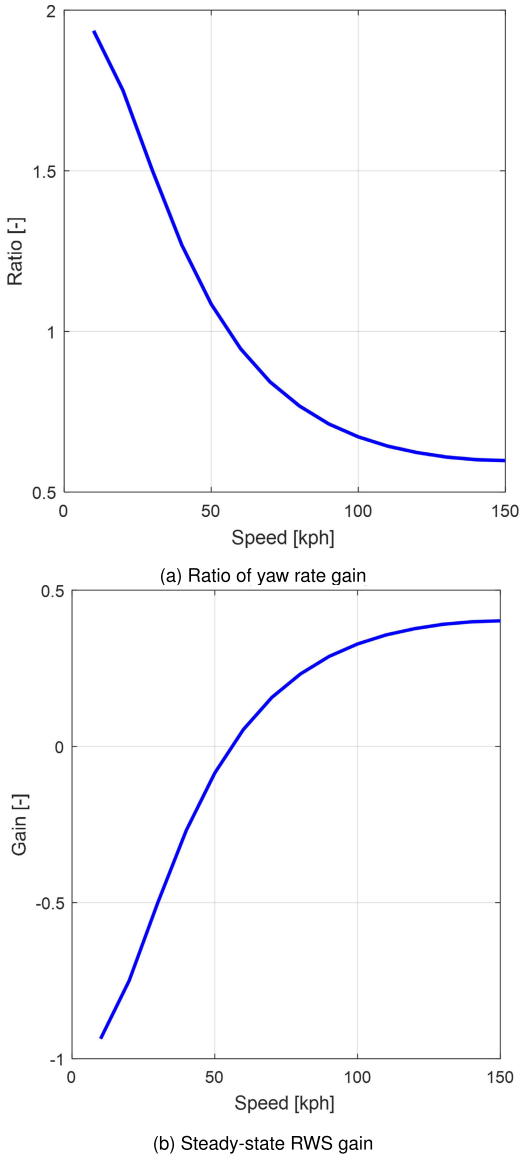

(a) Ratio of yaw rate gain

(b) Steady-state RWS gain

FIGURE 4. Illustration of the ratio of steady-state RWS gain obtained by numerical optimization. (a) Ratio of yaw rate gain $G^{\gamma}_{ss,RWS}/G^{\gamma}_{ss,FWS}$: as the ratio to the base vehicle is reduced vehicle speed increases. (b) Proportional gain k_δ: based on about 56 kph, RWS is controlled to be in-phase at high speed and reverse-phase at low speed.

the model-based feedforward control input is described. The goal of the transient RWS control is to enhance lateral transient response compared to the transient response when only steady-state control in (11) is exerted to the vehicle. For example, the goal of the transient control is to minimize yaw rate overshoot and unnatural lateral acceleration response. In this subsection, the proposed feedforward part of the transient control input will be presented first; subsequently, the closed-loop dynamics will be analyzed to investigate how such a control input affects the outcome.

The proposed RWS control input including the steady-state input and the feedforward part of the transient input is represented as follows:

$$\begin{aligned}\delta_r(t) &= \delta_{r,ss}(t) + \delta_{r,tr,ff}(t) \\ &= \underbrace{k_\delta \cdot \delta_f(t)}_{Steady-state} \\ &\quad + \underbrace{\left(\frac{1}{\eta}-1\right)\cdot\left\{(k_\delta-1)\cdot\delta_f(t)+K_{us}\cdot a_y(t)+\frac{L}{V_x(t)}\cdot\gamma(t)\right\}}_{Transient}\end{aligned} \tag{12}$$

where, $\delta_{r,tr,ff}$ is the feedforward control to modify transient characteristics of the rear-wheel steering vehicle.

The control law in (12) consists of two terms: the steady-state control input for modifying the steady-state yaw rate gain and the feedforward part for enhancing the vehicle's transient response. Note that the control law in (12) is the generalized control input of (11). This is because the control input in (12) becomes equal to the steady-state RWS of (11) when the design parameter becomes 1.

The effects of the control input (12) are analyzed. To analyze the effects of the control input in (12), the bicycle model in (3) is newly formulated in the form of the transfer function as follows:

$$\frac{\gamma(s)}{\delta_f(s)} = \frac{1}{\tau s+1}\cdot\frac{V_x}{L}\left[1-\frac{\delta_r(s)}{\delta_f(s)}-K_{us}\cdot\frac{a_y(s)}{\delta_f(s)}\right] \tag{13}$$

$$\tau = \frac{a_{11}}{a_{21}-|A|} = \frac{I_z V_x\left(C_f+C_r\right)}{C_f C_r L^2} \tag{14}$$

Here, a_{ij} is the element of matrix A at the i-th row and the j-th column, and |X| is the determinant of matrix X. The derivation of (13) and (14) are attached in Appendix A. As described in (13), the vehicle's yaw rate (or driver's steering angle) is regarded as the sole output (or input) of the system. The rear-wheel steering angle and the lateral acceleration is set as the external input of the system. Note that this system is a first-order delay system with the gain.

In the case of vehicles with the steady-state RWS control input only ($\delta_r = \delta_{r,ss}$), the lateral response can be expressed as follows:

$$\frac{\gamma(s)}{\delta_f(s)} = \frac{1}{\tau s+1}\cdot\frac{V_x}{L}\left[1-k_\delta-K_{us}\cdot\frac{a_y(s)}{\delta_f(s)}\right] \tag{15}$$

As mentioned above, the goal of the feedforward transient input is to enhance the transient response in (13). By substituting (12) into (13), the closed-loop dynamics with the control law in (12) can be derived as:

$$\frac{\gamma(s)}{\delta_f(s)} = \frac{1}{\eta\tau s+1}\cdot\frac{V_x}{L}\cdot\left[1-k_\delta-K_{us}\cdot\frac{a_y(s)}{\delta_f(s)}\right] \tag{16}$$

As described in (16), by changing the design parameter η, it is possible to modify the transient response of the vehicle lateral behavior. Since the parameter η is a coefficient of the time constant, the system becomes sluggish or responsive according to the value of such a parameter. We note that

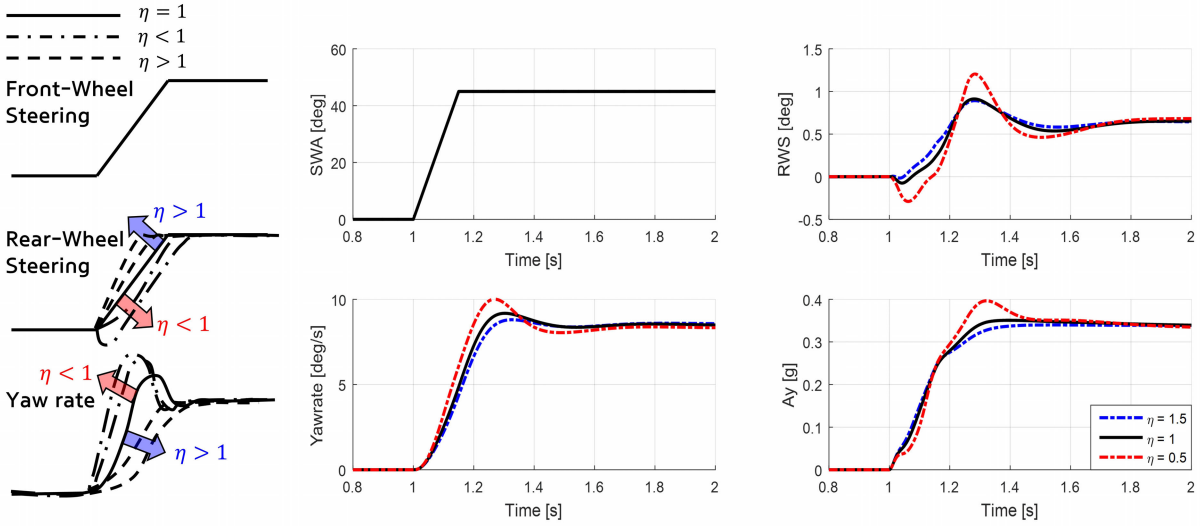

(a) Concepts of design paramter η (b) Verification of performance changes through simulation at 80kph, 45deg(300deg/s) step steer scenario

FIGURE 5. Comparison of vehicle response and rear-wheel steering input with changes.

the control input in (12) can modify the transient response of the vehicle without any information on tire and vehicle parameters.

Analysis of the design parameter η has been conducted via computer simulations. The trade-off relationship between the rise time and the overshoot was discovered via computer simulations. The conceptual figure and the simulation results are presented in Figure 5. Figure 5 (a) is a schematic diagram of the concept of the design parameter η. When η is bigger than 1, the system becomes sluggish: the rise time of yaw rate response is increased, and overshoot is decreased. On the other hand, the system becomes responsive when η becomes smaller than 1: The rise time in the transient region is improved. Moreover, the notable point in this case is the undershoot response of the rear wheel steering angle command. Figure 5 (b) shows the simulation results of changing the design parameter η revealing similarities with the conceptual diagram. The changes of η also affect the transient response of the lateral acceleration. The design of η is also aimed at modifying such a nonlinear transient response as shown in Figure 3. Based on these characteristics, η is tuned with reference to the optimal results in the step steer scenario such as the yaw rate's response time and the lateral acceleration's transient response.

Figure 6 shows the tuning results using (12) for mimicking the response time of the optimal RWS control's yaw rate. In the case of 30 kph presented in Figure 6 (a), the proposed control law (12) can imitate not only the response time but also the overshoot of the optimal yaw rate, by setting the design parameter $= 1.3$. In the case of 110 kph (Figure 6 (b)), the control law (12) can imitate the response time by setting the design parameter $= 0.6$. However, the overshoot increases noticeably. The overshoot must be reduced since the overshoot of the yaw rate response is

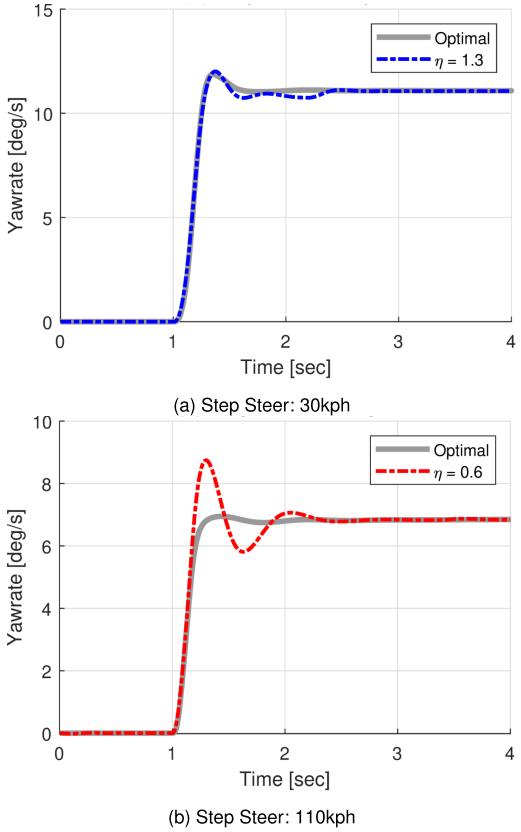

(a) Step Steer: 30kph

(b) Step Steer: 110kph

FIGURE 6. Selecting the design parameter η. (a) $\eta = 1.3$ to imitate the yaw rate's response time of optimal results at 30 kph. (b) $\eta = 0.6$ to imitate the yaw rate's response time of optimal results at 110 kph.

related to the lateral instability. Therefore, under high-speed driving, an additional control input is required to minimize the overshoot. The algorithm will be mentioned in detail in section 3.3.

C. REAR-WHEEL STEERING CONTROL FOR ENHANCED TRANSIENT HANDLING – FEEDBACK CONTROLLER

The feedback transient control input is proposed to compensate for the trade-off between the overshoot and response time that the feedforward transient control input has illustrated in Figure 5 and 6. Since the excessive overshoot of the yaw rate response in Figure 6 results from the side slip rate (the first time derivative of the side slip angle), the proposed feedback control is formulated as follows:

$$\begin{aligned}\delta_{r,tr,fb}(t) &= -K_{fb}\cdot V_x(t)\cdot\left(\dot{\beta}(t)-\dot{\beta}_{des}(t)\right)\\ &= -K_{fb}\cdot\left(a_y(t)-V_x(t)\cdot\gamma(t)\right)\end{aligned} \tag{17}$$

where $\delta_{r,tr,fb}$ is the feedback control to modify transient characteristics of the rear-wheel steering vehicle, and K_{fb} is the feedback gain that is a positive number. $\dot{\beta}$ is the time-derivative of the side slip angle, and $\dot{\beta}_{des}$ is the desired $\dot{\beta}$ that is zero in this paper.

The final form of the proposed control algorithm is obtained by adding (17) to (12) as follows:

$$\begin{aligned}&\delta_{r,proposed}(t)\\ &= \delta_{r,ss}(t)+\delta_{r,tr,ff}(t)+\delta_{r,tr,fb}(t)\\ &= \underbrace{k_\delta\cdot\delta_f(t)}_{Steady-state}\\ &\quad+\underbrace{\left(\frac{1}{\eta}-1\right)\cdot\left\{(k_\delta-1)\cdot\delta_f(t)+K_{us}\cdot a_y(t)+\frac{L}{V_x(t)}\cdot\gamma(t)\right\}}_{Feedforward\ for\ Transient}\\ &\quad\underbrace{-K_{fb}\cdot\left(a_y(t)-V_x(t)\cdot\gamma(t)\right)}_{Feedback\ for\ Transient}\end{aligned} \tag{18}$$

The proposed RWS algorithm determines the steady-state response using the yaw rate gain ratio, and modifies the transient response such as overshoot and peak response time by tuning η and K_{fb}. Yaw rate, lateral acceleration, and steering wheel angle in control law (18) are measured from sensors mounted on the vehicle. The vehicle longitudinal speed is estimated using the wheel speed and longitudinal acceleration [18].

Verification is required to ensure that the feedback control reduces the overshoot of the yaw rate without changing the steady-state yaw rate gain. The verification is processed in two parts: (1) the feedback control input does not change the steady-state yaw rate gain, and (2) the feedback control input reduces the overshoot.

First, (13) is reformulated by substituting (18) to identify whether the feedback gain changes the steady-state yaw rate gain.

$$\begin{aligned}\frac{\gamma(s)}{\delta_f(s)} &= \frac{1}{\eta_f\tau s+1}\cdot\frac{\eta_f}{\eta}\\ &\quad\times\frac{V_x}{L}\left[1-k_\delta-\left(K_{us}-\eta K_{fb}\right)\cdot\frac{a_y(s)}{\delta_f(s)}\right]\\ \eta_f &= \frac{\eta}{1+\frac{\eta K_{fb}V_x^2}{L}}\end{aligned} \tag{19}$$

Here, η_f is a function of η and K_{fb} that can express the yaw rate in the same way of (16). The derivation of (19) is attached in Appendix B. To obtain the steady-state yaw rate gain, (19) can be re-written as follows by applying $a_y = V_x\cdot\gamma_{ss}$ and the final value theorem:

$$\frac{\gamma_{ss}}{\delta_f} = \underbrace{\frac{V_x}{L+K_{us}\cdot V_x^2}}_{G^{\gamma}_{ss,FWS}}\cdot(1-k_\delta) = G^{\gamma}_{ss,RWS} \tag{20}$$

The results in (20) show that the steady-state yaw rate gain does not change even if the feedback control is added.

Second, this data verified that the feedback control in (17) reduces the overshoot. The transfer function of the closed-loop dynamics is derived by substituting (18) into (3) as follows:

$$\begin{aligned}\frac{\gamma}{\delta_f}(s) &= \frac{ps+q}{s^2+2\zeta\omega_n s+\omega_n^2}\\ where,\ p &= \frac{(k_\delta-1)\left(\frac{1}{\eta}-1\right)c_2}{1-c_1\left(\frac{1}{\eta}-1\right)K_{us}V_x+c_1V_xK_{fb}},\\ q &= \frac{(k_\delta-1)\left(\frac{1}{\eta}-1\right)\begin{vmatrix}C & A_1\end{vmatrix}}{1-c_1\left(\frac{1}{\eta}-1\right)K_{us}V_x+c_1V_xK_{fb}}\\ \omega_n^2 &= \frac{\left(\frac{1}{\eta}-1\right)\cdot\frac{|A|}{\begin{vmatrix}B & A_1\end{vmatrix}}\cdot\begin{vmatrix}A_1 & C\end{vmatrix}}{1-c_1\left(\frac{1}{\eta}-1\right)K_{us}V_x+c_1V_xK_{fb}}\\ 2\zeta\omega_n &= -\frac{N}{D}\\ N &= tr(A)+\left(\frac{1}{\eta}-1\right)K_{us}V_x\cdot\begin{vmatrix}A_2 & C\end{vmatrix}\\ &\quad+c_2\left(\frac{1}{\eta}-1\right)\frac{|A|}{\begin{vmatrix}B & A_1\end{vmatrix}}+V_xK_{fb}\begin{vmatrix}C & A_2\end{vmatrix},\\ D &= 1-c_1\left(\frac{1}{\eta}-1\right)K_{us}V_x+c_1V_xK_{fb}\end{aligned} \tag{21}$$

Here, ζ is the damping ratio of the system, and ω_n is the natural frequency of the system. Term c_i is the elements of the matrix C, and A_i is the i-th column vector of matrix A. |X| is the determinant of matrix X, and tr(X) is the trace of matrix X.

To verify that the overshoot in the step steer scenario is reduced, the yaw rate response in the step-steer scenario is derived by substituting $\delta_f(s) = k/s$ into (21). Term k is the step amplitude of steering command, and the value of k is SWA (45 deg) in this analysis.

$$\gamma(s) = \frac{kps+kq}{s\left(s^2+2\zeta\omega_n s+\omega_n^2\right)}$$

$$= \underbrace{\frac{kq}{\omega_n^2}}_{\gamma_{ss}} \cdot \left[\frac{1}{s} - \frac{s + \zeta\omega_n}{(s + \zeta\omega_n)^2 + \omega_d^2} - \left(\frac{\zeta\omega_n - \frac{p}{q}\omega_n^2}{\omega_d} \right) \cdot \frac{\omega_d}{(s + \zeta\omega_n)^2 + \omega_d^2} \right] \quad (22)$$

$$\gamma(t) = \gamma_{ss} \cdot \left[1 - e^{-\zeta\omega_n t} \cdot \cos\omega_d t - \left(\frac{\zeta\omega_n - \frac{q}{p}\omega_n^2}{\omega_d} \right) \cdot e^{-\zeta\omega_n t} \cdot \sin\omega_d t \right] \quad (23)$$

Here, γ_{ss} is the steady-state yaw rate ($k \cdot G^{\gamma}_{ss,RWS}$) in the step steer scenario, and ω_d is the damped natural frequency of the system ($\omega_n \cdot \sqrt{1-\zeta^2}$). Expression (23) is obtained by transforming (22) from the s-domain to the t-domain.

For a given step steering input, the overshoot of the yaw rate is calculated as $Overshoot = \frac{(\gamma_{max} - \gamma_{ss})}{\gamma_{ss}} \times 100[\%]$, and the peak response time is calculated as $t_{\gamma,resp} = t_{\gamma,\max} - t_{\delta_{SWA,50\%}}[sec]$. Term $t_{\delta_{SWA,50\%}}$ denotes the time required for the steering wheel angle rise from 0% to 50%. Reducing overshoot is equivalent to reducing the peak value (i.e. maximum value, γ_{max}) of the yaw rate. Likewise, since $t_{\delta_{SWA,50\%}}$ is fixed, reducing the peak response time $t_{\gamma,resp}$ is equivalent to reducing the peak time $t_{\gamma,max}$.

$$\begin{aligned} \text{Reducing } t_{\gamma,resp} &\Leftrightarrow \text{Reducing } t_{\gamma,\max} \\ \text{Reducing } Overshoot &\Leftrightarrow \text{Reducing } \gamma_{\max} \end{aligned} \quad (24)$$

The peak time can be obtained by differentiating (23), and the peak value of the yaw rate can be obtained by substituting the peak time again into (23).

$$\begin{aligned} \frac{d\gamma}{dt}(t_{\gamma,\max}) &= 0 \\ \gamma(t_{\gamma,\max}) &= \gamma_{\max} \end{aligned} \quad (25)$$

The relationship between the peak time/yaw rate and the feedback gain is numerically analyzed. The peak time and the peak yaw rate at 110 kph of vehicle speed were calculated from (25). The peak response time and overshoot are shown in Figure 7. The yaw rate overshoot monotonically decreases as the feedback gain K_{fb} increases. However, the relationship between $t_{\gamma,resp}$ and the feedback gain is a convex function, and (K_{fb}, $t_{\gamma,resp}$) = (0.016, 0.17) is a local minimum point. Since minimizing both the overshoot and the peak response time is the goal of the control design, the feedback gain K_{fb} is set to 0.016 in the step steer scenario at the 110 kph vehicle speed. The 'X' mark indicates the proposed feedback gain in this case.

Figure 8 represents the locus of the closed-loop poles of the transfer function (21) and indicates the yaw rate response to the driver's steering input. The feedback gain K_{fb} varies from 0 to 0.05 under the condition that is dry asphalt ($\mu = 1$) at high-speed (110 kph). Figure 8 (a) shows the root-locus plot [19]–[21] of the proposed RWS algorithm. Figure 8 (b) shows the change of the poles with respect to the change of the feedback gain in the log scale x-axis. As the feedback gain K_{fb} increases, the pole first moves towards

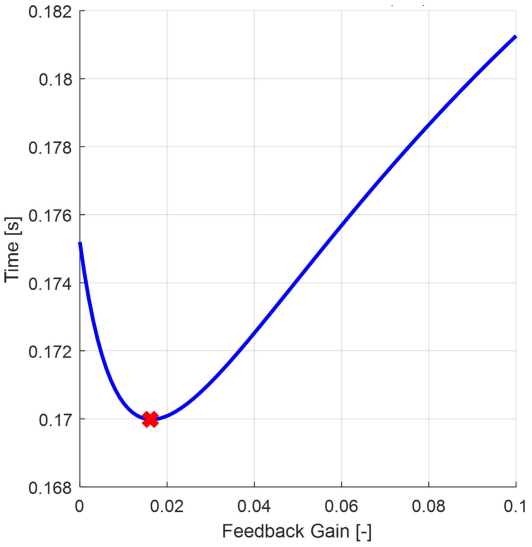

(a) Peak response time

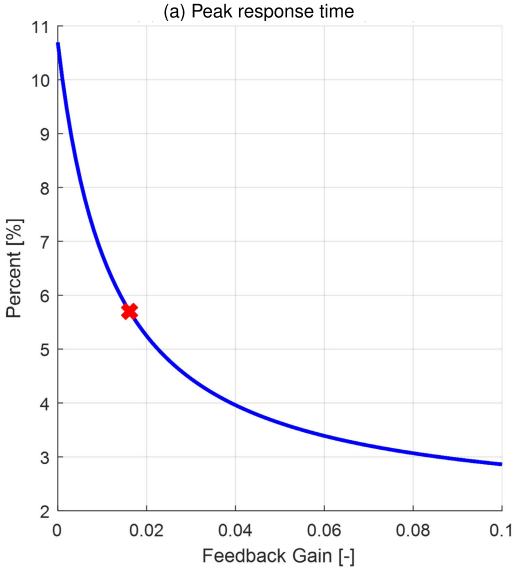

(b) Overshoot of yaw rate

FIGURE 7. Illustration of peak response time and overshoot in step steer scenario at 110 kph, 45 deg (300 deg/s), dry asphalt, with vehicle parameters in Table 1. (a) peak response time ($t_{\gamma,resp}$): as feedback gain increases, the peak response time of yaw rate is reduced. (b) overshoot (%OS): as feedback gain increases, the overshoot of yaw rate is reduced.

the left-hand plane (LHP; Figure 8 (a)) but the poles bifurcate around $K_{fb} = 0.032$ as illustrated in Figure 8 (a) and (b). The feedback gain of the proposed algorithm is determined by the process shown in Figure 7 and places the poles before the bifurcation [22], [23]. Figure 8 (a) shows that the feedback control increases the damping ratio ζ from 0.16 to 0.6. This means that the feedback control is effective for overshoot reduction. In Figure 8 (b), the feedback control places the real part of the poles from -0.1 to -0.3. This means that the feedback control improves the stability of the RWS control system.

The blue solid line in Figure 8. (b) indicates the pole changes when the tire cornering stiffnesses are

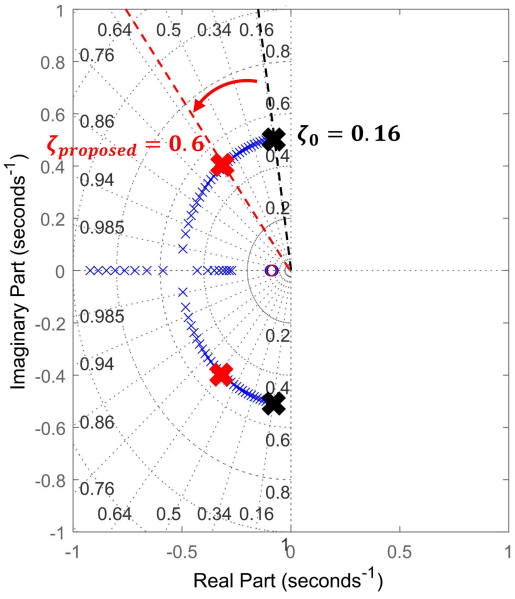

(a) Root-locus plot of proposed RWS

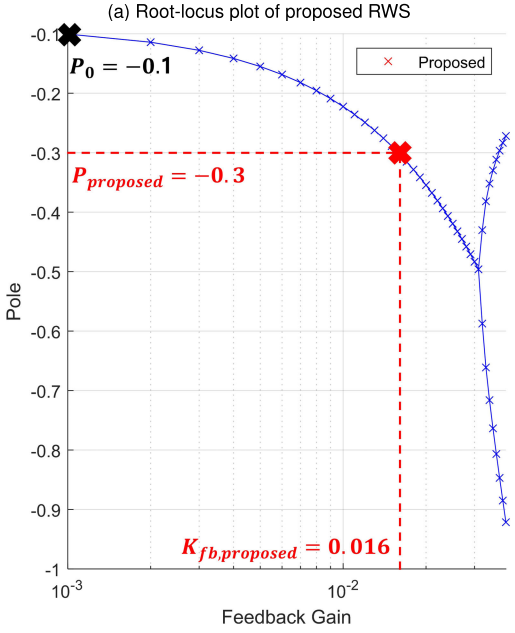

(b) Closed-loop poles associated with feedback gain

FIGURE 8. Root-Locus of Proposed RWS algorithm at 110 kph, dry asphalt, with vehicle parameters in Table 1.

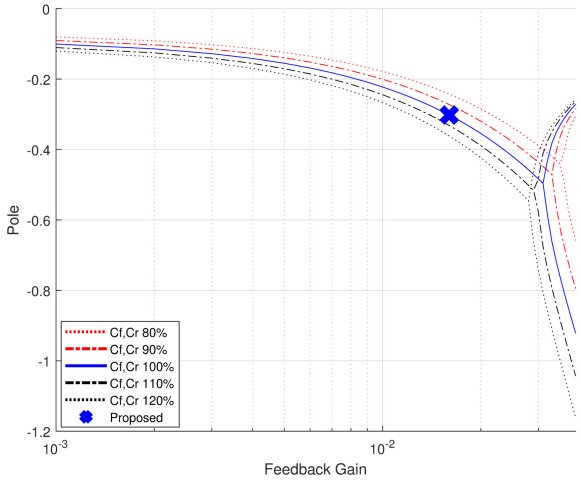

FIGURE 9. Poles versus feedback gain for tire parameter variations. Step steer (45 deg, 300 deg/s) at 110 kph.

$C_f = 20000$ N/rad and $C_r = 26800$ N/rad, which are the linear cornering stiffnesses of the test vehicle. The linear cornering stiffnesses nicely represent the vehicle's lateral dynamics in mild driving region. However, the tire cornering stiffness can be changed during driving according to vehicle states, tire states, road friction, etc. The closed-loop poles' change under such a condition was investigated to analyze the control performance under varying tire stiffnesses conditions.

Figure 9 shows a closed-loop pole change regarding the tire cornering stiffness variation based on (21). As illustrated in Figure 9, the value of the closed-loop poles increases as the tire cornering stiffnesses increase. This is because increased tire stiffness increases the natural frequency of the closed-loop system. Moreover, the data suggest that the poles are still present on the left-hand plane (stable closed-loop poles) regardless of the tire cornering stiffness.

The best feedback gain is changed regarding vehicle speed as illustrated in Figure 10. Figure 10 (a) shows the feedback gain with vehicle speeds obtained via the same process as in Figure 7. At low speeds (below 56 kph), the feedback gain is set to 0 because additional feedback control increases the peak yaw rate response time. The detailed process of determining the feedback gain at low speeds can be found in Appendix C. The feedback gain is increased as vehicle speed increases at high speeds (over 56 kph).

Figure 10 (b) displays the value of the design parameter η. Section 3.2 shows that in the low speed region, the yaw rate response of the optimal solution can be imitated only by adopting the design parameter η. Therefore, the design parameter η is adjusted to mimic the optimal solution while the feedback gain is set to zero. However, both the design parameter η and the feedback gain must be tuned to mimic the optimal solution at high speed. At high speeds, η is adjusted to show a similar performance with the optimal solution when the feedback gain is set to Figure 10 (a).

Figure 11 shows the performance of the proposed algorithm in (18). The proposed algorithm in (18) is compared with control inputs in (8) and (12) and the optimal solution. The simulation scenario is a 45 deg (300 deg/s) step steer at 110 kph vehicle speed on the dry asphalt. 'Feedforward' in Figure 11 stands for the control input in (12) with $\eta = 0.6$. 'Proposed' is the control input in (18) with $(\eta, K_{fb}) = (0.8, 0.016)$. Feedback using (η, K_{fb}) noticeably reduces the overshoot of yaw rate to 13.07%, while feedforward using η changed the results by 40.14%. Moreover, $\delta_{r,tr,fb}$ in (17) acts as a side slip angle feedback control as illustrated in Figure 11, and it helps the

TABLE 2. Performance evaluation indices.

Scenario	Performance index	Calculation
Step steer	Overshoot	$Overshoot = \frac{\gamma_{max} - \gamma_{ss}}{\gamma_{ss}} \times 100\ [\%]$
	Peak Response Time	$t_{\gamma.resp} = t_{\gamma.max} - t_{\delta_{SWA\ .50\%}}\ [sec]$
	TB Factor	$\mathrm{TB} = t_{\gamma.resp} \times \beta_{ss}\ [\mathrm{sec} \cdot \mathrm{deg}]$
	Yaw rate Gain	$\frac{\gamma_{ss}}{\delta_f}\ [1/s]$

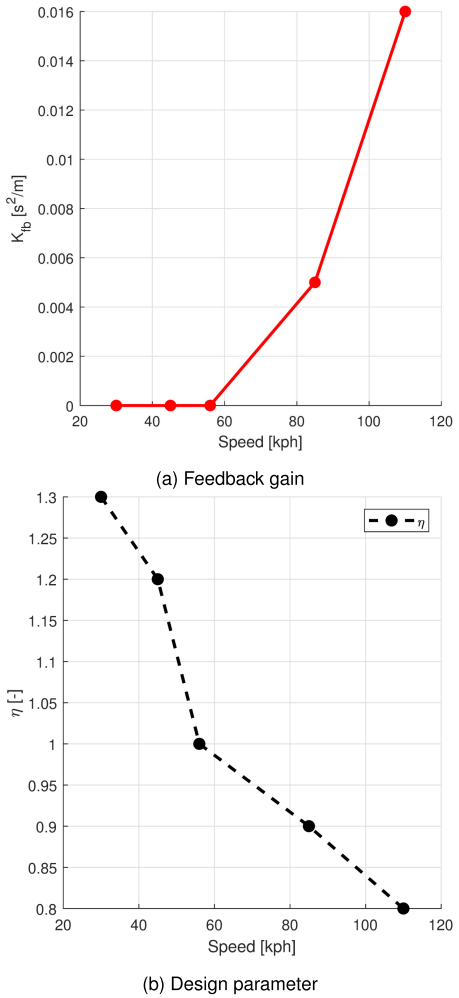

FIGURE 10. Changes of feedback gain and design parameter η with vehicle speed. (a) Feedback gain (K_{fb}): the feedback gain is increased as vehicle speed increases. (b) Design parameter (η): the design parameters are reduced as vehicle speed increases.

feedforward control to converge quickly in controlling the steady-state side slip angle to zero. Moreover, the RWS of the proposed algorithm was initially steered to the opposite direction of the front steer angle as shown in Figure 11 (a). This initial undershoot command of the proposed algorithm is identical to the RWS command of the optimal solution.

IV. SIMULATION RESULTS

The simulation results provide analysis and understanding to investigate the performance of the proposed algorithm. Three simulation results were performed in this paper. First, the step steer scenario based-on ISO-7401 was conducted to compare the optimal control results. The comparison results are evaluated whether the proposed control algorithm implements the optimal performance with overshoot, response time, and TB factor as the objective criteria [24]–[27]. Second, the proposed control algorithm is verified in that it performs well even in the sine with dwell scenario. Third, the robustness of the proposed control algorithm is investigated for low friction road conditions. These simulations are compared with three different controllers: 1) Base vehicle, F-segment sedan with Rear-Wheel Drive (RWD); 2) Proportional RWS controller with the gain expressed as a function of vehicle speed in Figure 4; and 3) Optimal RWS controller calculated by offline numerical optimization.

A. OPEN-LOOP STEERING COMMAND – STEP INPUT

The proposed RWS control algorithm is carried out to emulate the lateral behavior of a reference model. The reference model is conducted based on the offline numerical optimization of [6]. The numerical optimization is simulated through open-loop maneuvers that do not involve the driver's intention. In this section, a step steer scenario is adopted that satisfies the ISO-7401 with a 45 deg steering wheel angle and a 300 deg/s steering rate. The optimal control (i.e. RWS^{V_y} control of [6]) is compared with the passive vehicle (only FWS) through objective criteria such as overshoot, response time, and TB factor [23]–[26] of the following Table 2.

Here, $\gamma_{\max}$ is the maximum value of yaw rate, and β_{ss} is the steady-state value of side slip angle. $t_{\gamma,max}$ is the time required for the response to reach the first peak of the overshoot, and $t_{\delta_{SWA,50\%}}$ is the time required for the steering wheel angle rise from 0% to 50%; it serves as a reference point in calculating

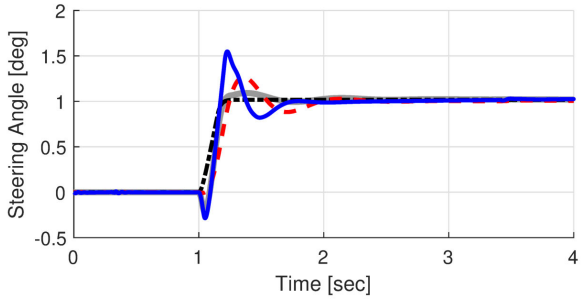

(a) Rear-wheel steering angle

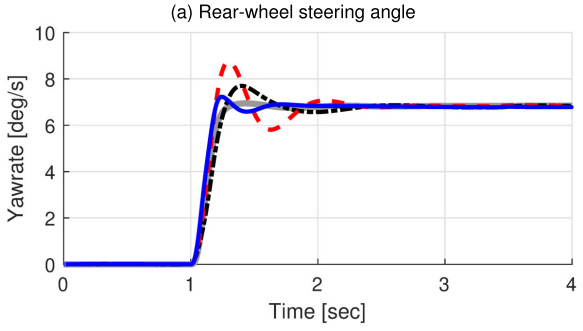

(b) Yaw rate

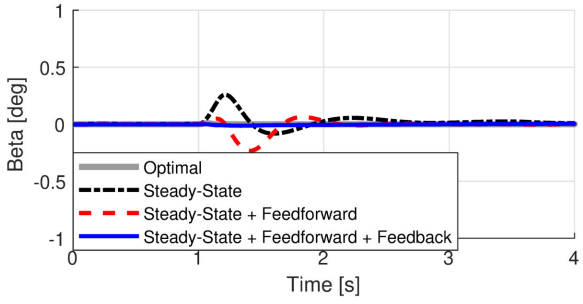

(c) Side slip angle

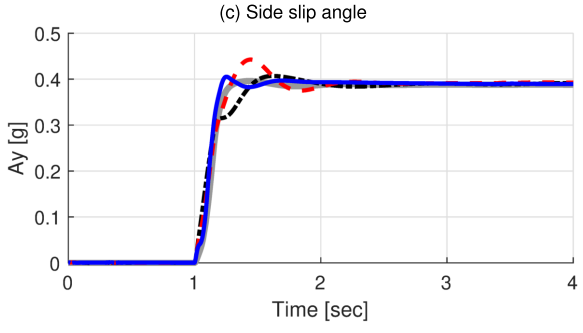

(d) Lateral acceleration

FIGURE 11. Effect of feedback controller with $k_\delta = 0.357$, for step steer at 110 kph, 45 deg (300 deg/s), dry asphalt.

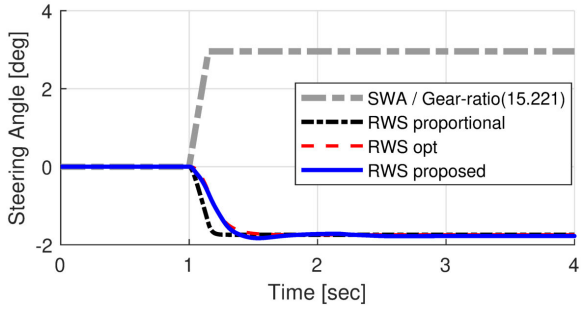

(a) Steering angle

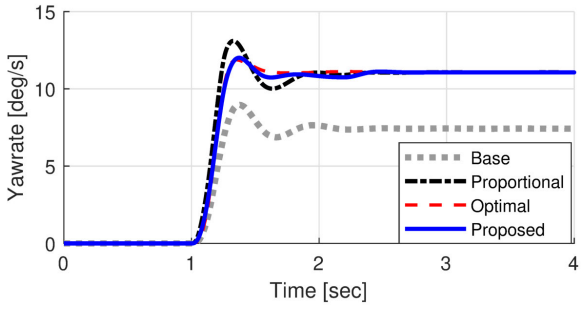

(b) Yaw rate

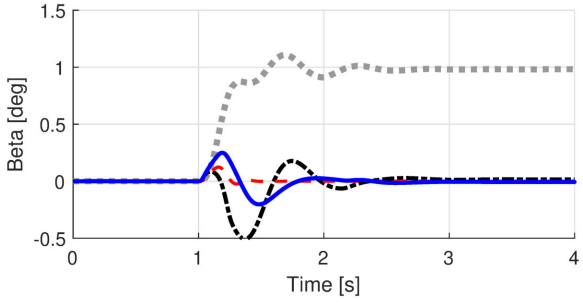

(c) Side slip angle

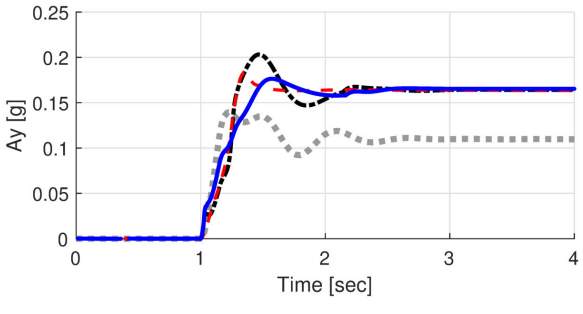

(d) Lateral acceleration

FIGURE 12. Result of step steer at 30 kph, 45 deg (300 deg/s), dry asphalt, with $k_\delta = -0.501$, $\eta = 1.3$, $K_{fb} = 0$.

the peak response time $t_{\gamma,resp}$. The primary concern in this section is to assess how well the proposed control algorithm implements the best performance of the numerical optimization based on objective criteria.

Figures 12 and 14 (a) are simulation results and performance assessment graphs at low speeds. Figure 12 (a) shows "SWA/Gear-ratio (15.221)": This means the steering command divided by the gear ratio of vehicle, and it represents the front-wheel steering input by the driver. Steady-state control gain and transient control gains are set for emulating the target behavior of the optimal control. These are designated as $(k_\delta, \eta, K_{fb}) = (-0.501, 1.3, 0)$. The performance assessment graph in Figure 14 (a) shows that the RWS control at low speeds improves vehicle maneuverability by increasing the steady-state yaw rate gain from 0.16 [1/s] to 0.25 [1/s]. The rear-wheel steering is controlled in the opposite direction to the front-wheels, which increases the yaw rate gain to make the TB factor zero. Vehicles with RWS control input (proposed, optimal, proportional) reduce the peak response

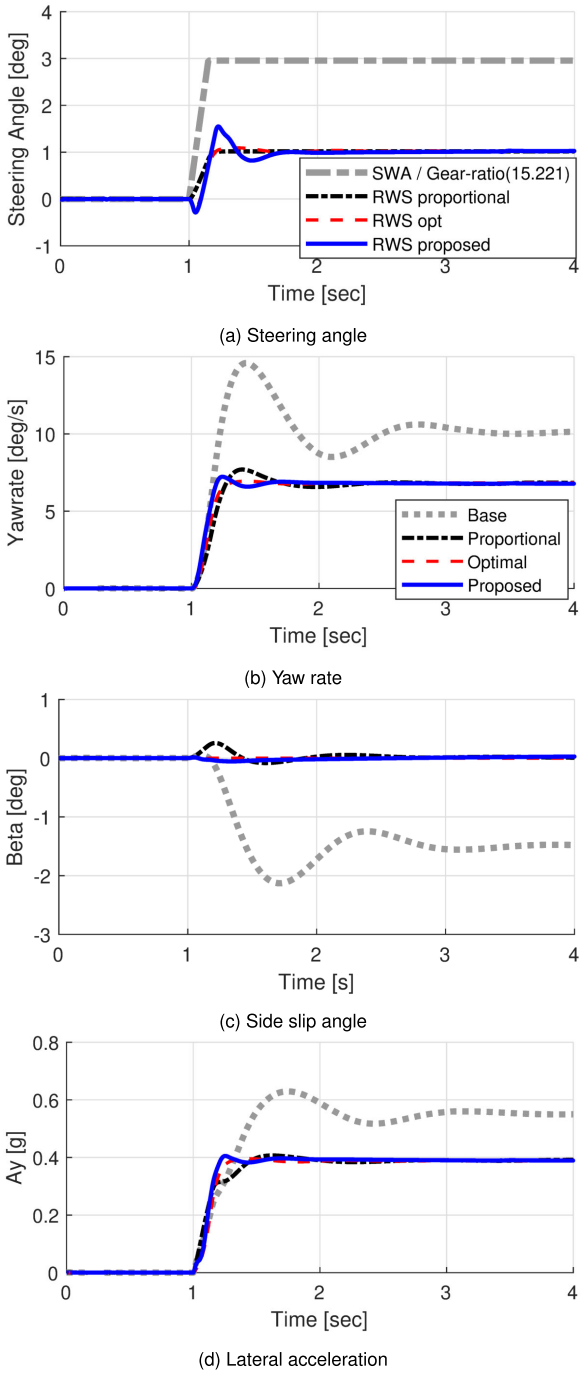

FIGURE 13. Result of step steer at 110 kph, 45 deg (300 deg/s), dry asphalt, with $k_\delta = 0.357$, $\eta = 0.8$, $K_{fb} = 0.016$.

time from 0.31 s to 0.26 s compared to the base vehicle. In terms of overshoot, performance is evaluated as follows: optimal (7.1%) âLđ'proposed (7.4%) ≪ proportional (18.5%) < base (20.9%). From an overall perspective, the proposed RWS control algorithm at low speeds shows better performance compared to the proportional control and base, and the proposed algorithm emulates the optimal results very well.

Figures 13 and 14 (b) illustrate the simulation results and performance assessment at high speed. Steady-state control gain and transient control gains are set to emulate the target behavior of the optimal control. These values are designated as (k_δ, η, K_{fb}) = (0.357, 0.8, 0.016, respectively). The rear-wheel steering is controlled in the same direction to front-wheels, which decreases the yaw rate gain to make the TB factor zero. The proposed algorithm is slightly insufficient to mimic the optimal control's overshoot, but greatly reduces overshoot compared to the proportional and base vehicle. On the other hand, the proposed algorithm shows the fastest response (0.17 s) in terms of peak response time.

The simulation results can be explained in the physical analysis and control design point of view. From the physical analysis viewpoint, one sees a difference in RWS command. Compared to the optimal control, input-delay due to the initial undershoot is similar, but it shows that the proposed algorithm subsequently has an overshoot-shaped control input. This results in greater lateral forces on the rear-axle creating a faster yaw rate response. From the control design point of view, the feedback control reduces the overshoot and peak response time compared to the feedforward control. Figure 7 illustrates that the proposed algorithm has a faster response than the optimal result by further reducing the peak response time using the feedback control. Furthermore, as shown in Figure 13 (d), the optimal control and the proposed algorithm has a linear transient response of the lateral acceleration while the proportional control has a nonlinear (stair-shaped) transient response. Additionally, the proposed algorithm converges the side slip angle to zero better than the base and the proportional control. In this regard, the proof of stability has been attached in the Appendix D.

Figure 15 shows the performance indices throughout the driving region: from low to high lateral acceleration. These results are obtained by increasing the amplitude of step steering input at 110 kph. Figure 15 (a) shows the changes of the yaw rate overshoot. The base vehicle's overshoot exceeds 30%, and the proportional controller's overshoot rises to 27% as the lateral acceleration increases. The proposed algorithm also increases the overshoot by more than 10% in limit handling (Ay>0.6g), but it shows good performance in mild driving (Ay<0.6g) by maintaining the overshoot less than 10%. Figure 15 (b) represents the peak response time according to the lateral acceleration. Compared to the proportional controller exceeded 0.25 s, the proposed algorithm maintains below 0.2 s from mild driving to limit handling. Figure 15 (c) represents the changes in TB factor. In limit handling, the RWS vehicles minimize the side slip angle by maintaining below 0.2 deg·s while the base vehicle increases a TB factor to more than 1 deg·s.

B. OPEN-LOOP STEERING COMMAND – SINE WITH DWELL

The proposed control algorithm has been simulated to verify whether it performs well for the sine with dwell scenario. The steering input is configured as 0.4 g/0.8 g Ay level

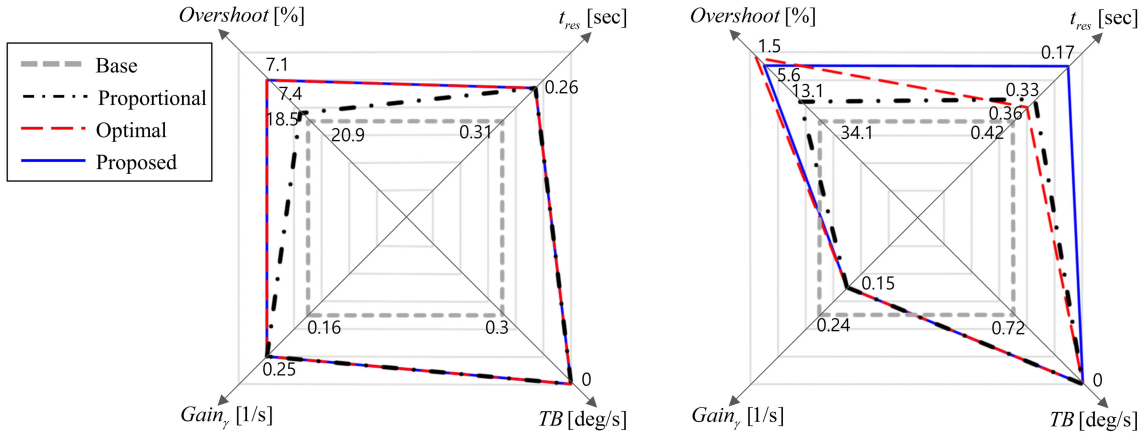

(a) Web assessment: Step 30kph

(b) Web assessment: Step 110kph

FIGURE 14. **Web assessment for comparison with the optimal performance.**

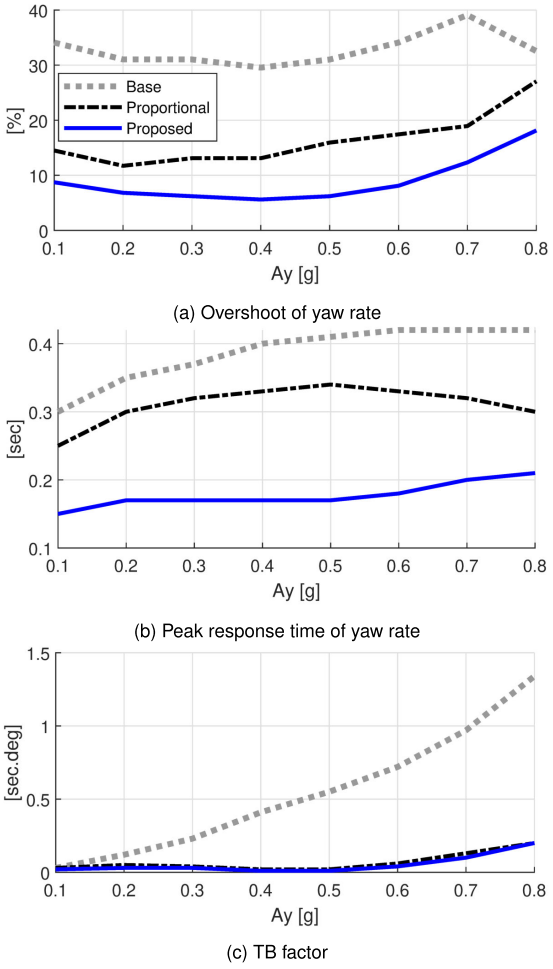

(a) Overshoot of yaw rate

(b) Peak response time of yaw rate

(c) TB factor

FIGURE 15. **Performance indices throughout the driving region: from low to high lateral acceleration.**

in the first peak. This is based-on ISO-19365 (sine wave of 0.7 Hz frequency, 500 ms delay at the dwelling zone). The performance test is conducted with the previously set η and K_{fb}. This result comparison was conducted for the following three controlled vehicles: base, proportional, and proposed. The purpose of this section is to identify the effect of RWS intervention and transient controller on vehicle stability.

Figure 16 shows the simulation results for the sine dwell test with Ay 0.4 g level. The vehicle speed is 110 kph, and SWA for a 0.4g level of Ay requires about 25 deg for the base vehicle and about 45 deg for the RWS vehicles. Figure 16 (b) shows that the proposed algorithm has a linearity yaw rate response to the driver's steering input in the dwelling area (2.5 s – 4 s). The proposed algorithm then shows a quick convergence and a smaller overshoot compared to other vehicles. Comparing the side slip angle in Figure 16 (c), one sees that the proposed algorithm significantly reduces below 0.09 deg while the base vehicle produces a side slip angle of up to 1.2 deg; the proportional controller produces a value up to 0.24 deg. Additionally, the proposed algorithm has the smallest rate of change in the side slip angle. This can be seen in the graphs of yaw rate and lateral acceleration. The proposed algorithm shows that the first peak time of yaw rate and lateral acceleration are almost the same, while the base and proportional control have a time gap. This result is explained by the effect of the feedback control in (17).

Figure 17 represents the simulation results for the sine dwell test at Ay 0.8g level where the base vehicle spins out. The vehicle speed is 110 kph and SWA for 0.8g level of Ay requires about 55 deg for the base vehicle and about 100 deg for RWS vehicles. For a mild maneuver (Ay 0.4g level), the proposed algorithm has a similar performance in limit handling maneuver (Ay 0.8g level). Thus, it can be seen that the proposed algorithm, tuned to emulate the optimal control to minimize side slip angle for step steer, performs the control objective well for other steering inputs.

C. PERFORMANCE COMPARISON ON A LOW FRICTION ROAD

The robustness of the proposed RWS algorithm has been investigated for low tire-road friction cases. In contrast to the

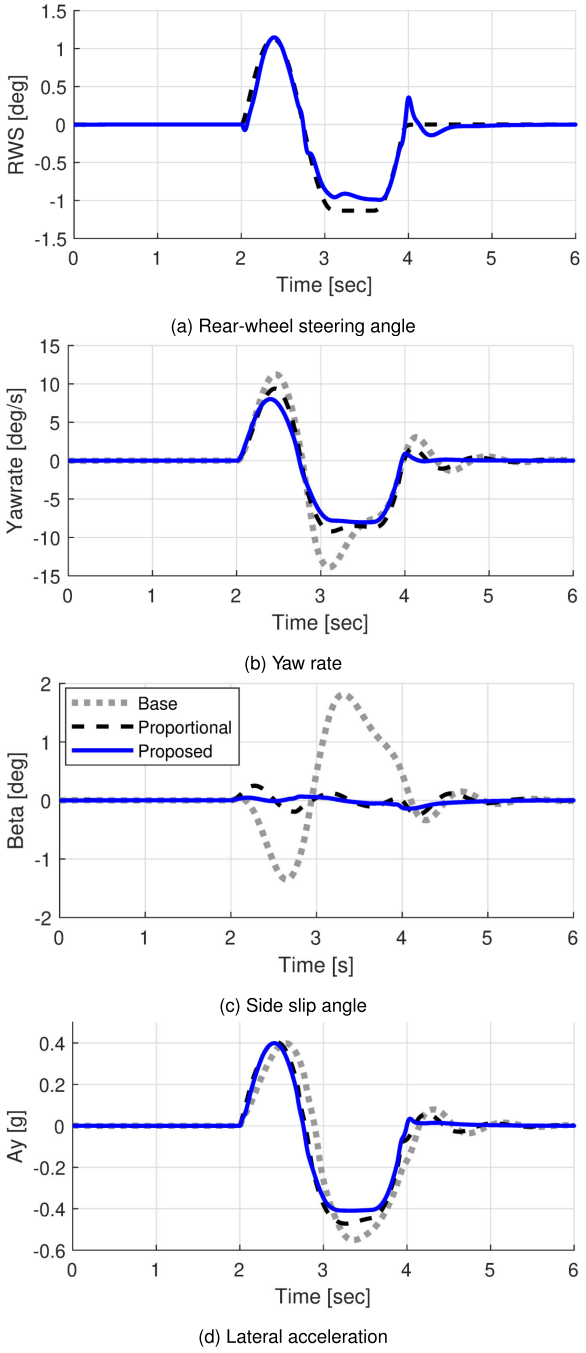

FIGURE 16. Result of sine dwell at 110 kph, peak Ay 0.4g, dry asphalt, with $k_\delta = 0.357$, $\eta = 0.8$, $K_{fb} = 0.016$.

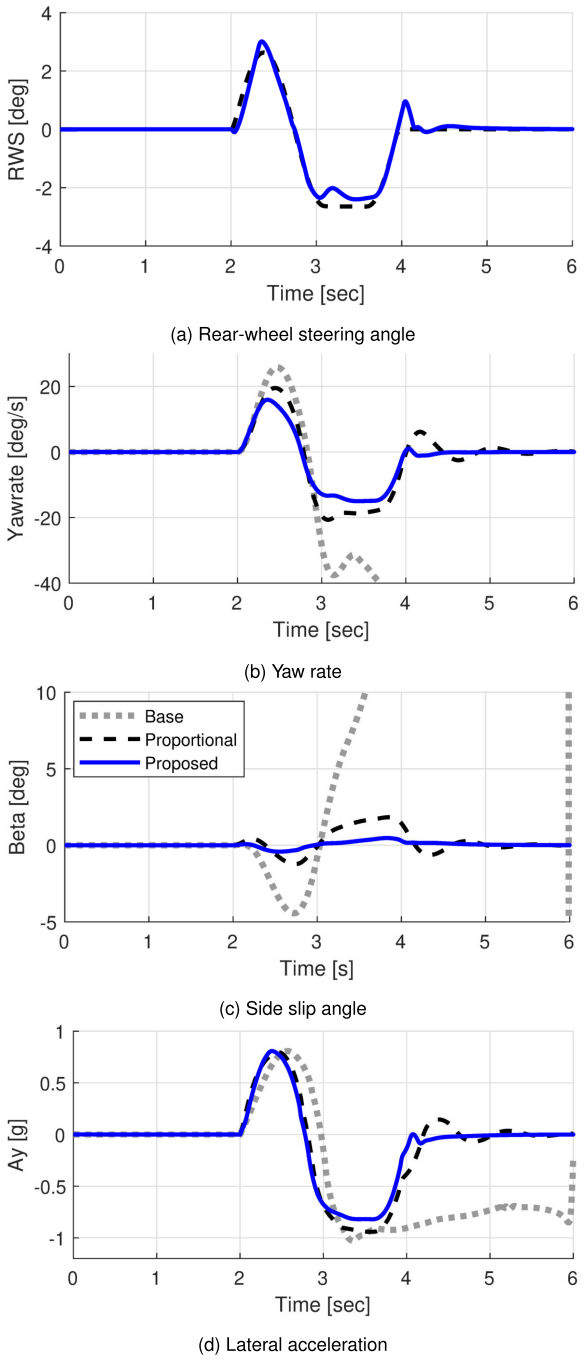

FIGURE 17. Result of sine dwell at 110 kph, peak Ay 0.8g, dry asphalt, with $k_\delta = 0.357$, $\eta = 0.8$, $K_{fb} = 0.016$.

results in section 4.1 where the RWS controlled vehicle performs the optimal performance on high friction roads ($\mu = 1$), this section shows what happens to RWS performance when the road surface condition is changed to low friction roads ($\mu = 0.3$). The performance of the proposed RWS control algorithm has been compared to the base vehicle, the steady-state control input in (11), and the feedforward control without feedback control in (12). The simulation was conducted to investigate the performance of the proposed algorithm for the following scenarios: step steer (45 deg, 300 deg/s) and sine with dwell (0.3g level of the first peak Ay).

Figure 18 illustrates the performance changes of RWS controllers when driving on a low friction road. The base vehicle spins out and has a loss of stability. In the case of the steady-state control and the feedforward control tuned on high friction roads, the yaw rate and side slip angle of the vehicle did not diverge but oscillated over a large period. In the case of the proposed algorithm, the algorithm

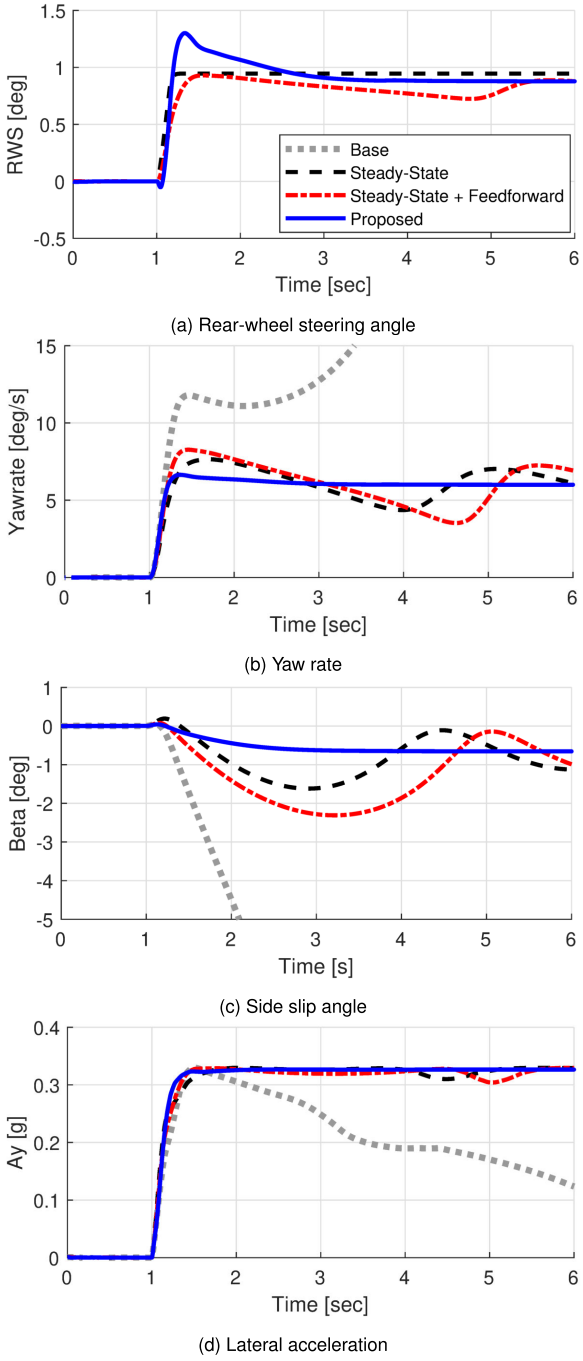

FIGURE 18. Step steer at 110 kph, 45deg (300deg/s), icy asphalt, with $k_\delta = 0.357$, $\eta = 0.8$, $K_{fb} = 0.016$.

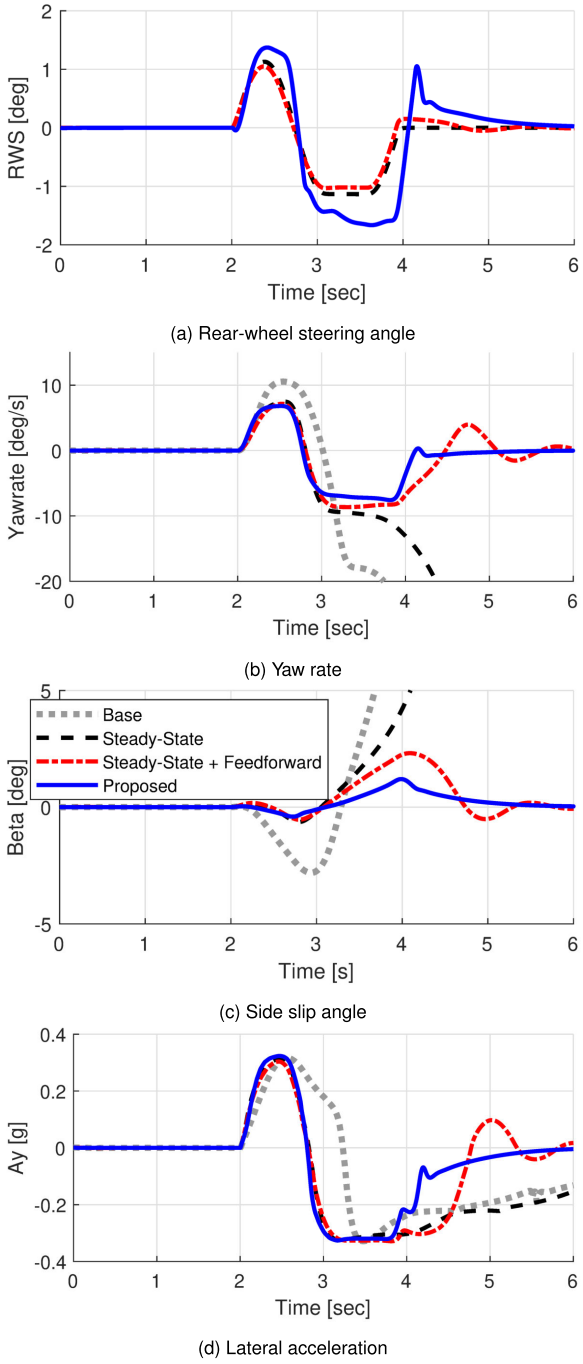

FIGURE 19. Sine with dwell at 110 kph, peak Ay 0.3g, icy asphalt, with $k_\delta = 0.357$, $\eta = 0.8$, $K_{fb} = 0.016$.

tuned on dry asphalt has a 0.5 deg offset in side slip angle, but it converges fast. Compared to the dry asphalt results (Figure 12 - 13), the proposed algorithm has the following features: slightly increased overshoot (7.4% to 10.5%) and peak response time (0.26 s to 0.28 s); this is superior to other controllers. In terms of lateral acceleration, the proposed algorithm maintains the linear shape response in the transition area while the steady-state control has a nonlinear shape.

Figure 19 shows the results of sine with dwell scenario on the icy asphalt driving condition. The base vehicle and the steady-state control tuned on high friction roads lead to spin out and loss of lateral stability. The feedforward and the proposed RWS algorithm do not diverge. Compared to dry asphalt results (Figure 15 - 16), the RWS input of the proposed algorithm on the low friction road differs remarkably from RWS input of the steady-state control. This difference

results from the feedback controller that improves the vehicles' lateral stability.

V. CONCLUSION

A new rear-wheel steering control method to enhance the vehicle handling characteristics without any information on tire characteristics parameters has been presented. The proposed algorithm consists of the steady-state and transient control input. The steady-state control input is proportional to the driver's front-wheel steering. The proportional gain is pre-determined as a function of vehicle speed using the offline optimization results, which is designed to minimize vehicle lateral velocity. The transient control input enhances the lateral transient response of the vehicle's yaw rate and lateral acceleration, and is designed as a combination of the feedforward and feedback inputs. In the feedforward input, a new feedforward gain is introduced to adjust the transient response of the vehicle's yaw rate. The feedback input significantly reduces the yaw rate overshoot via the first-time derivative of the vehicle side slip angle.

Computer simulations were used to evaluate the proposed control algorithm and were compared with three different control systems: (1) base (passive) vehicle; (2) proportional RWS system with the pre-determined rear-to-front steering ratio that is a function of the vehicle speed; and (3) optimal RWS system obtained by offline numerical optimization. The simulation results show that the proposed algorithm nicely emulates the optimal handling performance for step steer scenarios without any information on tire parameters. Moreover, compared to the other RWS control algorithms, the proposed control algorithm shows superior performance in the vehicle's lateral stability and maneuverability even under various steering and road surface conditions.

Since the proposed RWS control algorithm exhibits good performance at the simulation level, the rear-wheel steering control algorithm for the target vehicle could be developed via a real-time software tool. Real-time implementation and vehicle tests for the evaluation of this algorithm are the topics of our future research.

APPENDIX A
DERIVATION PROCESS OF (13)

In (3) representing the vehicle bicycle model, summarizing in the direction of eliminating the side slip angle β is as follows:

$$\frac{a_y}{V_x} = \dot{\beta} + \gamma = a_{11}\beta + (a_{12}+1)\,\gamma + b_1\delta_f + c_1\delta_r \quad \text{(A.26)}$$

$$\beta = \frac{1}{a_{21}} \cdot \left(\dot{\gamma} - a_{22}\gamma - b_2\delta_f - c_2\delta_r\right) \quad \text{(A.27)}$$

where, a_{ij} is the element of matrix A at the i-th row and the j-th column, and b_i, c_i are the elements of the matrices B and C, respectively. Equation (A.26) represents the ratio of the lateral acceleration to the vehicle speed using the first row of (3). Equation (A.27) is the second row of (3) and is used for canceling the side slip angle in (A.26). The lateral dynamics can be expressed with the measurable vehicle signals such as yaw rate and lateral acceleration, as shown in (A.28) below:

$$\begin{aligned} a_{11}\dot{\gamma} + (a_{21} - |A|)\cdot\gamma &= a_{21}\cdot\frac{a_y}{V_x} + |A_1\ B|\cdot\delta_f \\ &\quad + |A_1\ C|\cdot\delta_r \\ |A| &= \begin{vmatrix} a_{11} & a_{12} \\ a_{21} & a_{22} \end{vmatrix}, \\ |A_1\ B| &= \begin{vmatrix} a_{11} & b_1 \\ a_{21} & b_2 \end{vmatrix}, \\ |A_1\ C| &= \begin{vmatrix} a_{11} & c_1 \\ a_{21} & c_2 \end{vmatrix} \end{aligned} \quad \text{(A.28)}$$

where, A_i is the i-th column vector of matrix A, and |X| is the determinant of matrix X. Equation (A.28) can be transformed from the time domain (real variable t) to the frequency domain (complex variable s) by Laplace transformation. The process of expressing the vehicle lateral response is as follows:

$$\begin{aligned} &\{a_{11}s + (a_{21} - |A|)\}\cdot\gamma(s) \\ &\quad = a_{21}\cdot\frac{a_y(s)}{V_x} + |A_1\ B|\cdot\delta_f(s) + |A_1\ C|\cdot\delta_r(s) \end{aligned} \quad \text{(A.29)}$$

$$\begin{aligned} &\frac{\gamma(s)}{\delta_f(s)} \\ &\quad = \{a_{11}s + (a_{21} - |A|)\}^{-1} \\ &\qquad \times\left[|A_1\ B| + |A_1\ C|\cdot\frac{\delta_r(s)}{\delta_f(s)} + \frac{a_{21}}{V_x}\cdot\frac{a_y(s)}{\delta_f(s)}\right] \\ &\quad = \frac{1}{\tau s+1}\cdot\frac{V_x}{L}\left[1 - \frac{\delta_r(s)}{\delta_f(s)} - K_{us}\cdot\frac{a_y(s)}{\delta_f(s)}\right] \end{aligned} \quad \text{(A.30)}$$

APPENDIX A-1
LATERAL RESPONSE OF (16)

By substituting equation (12) into equation (13), vehicle lateral response of the proposed algorithm is derived as follows:

$$\begin{aligned} \frac{\gamma(s)}{\delta_f(s)} &= \frac{1}{\tau s+1}\cdot\frac{V_x}{L} \\ &\quad \times\left[1 - \frac{k_\delta}{\eta} - 1 + \frac{1}{\eta} - \left(\frac{1}{\eta} - 1\right)\cdot K_{us}\cdot\frac{a_y(s)}{\delta_f(s)}\right. \\ &\quad \left. - \left(\frac{1}{\eta} - 1\right)\cdot\frac{L}{V_x}\cdot\frac{\gamma(s)}{\delta_f(s)} - K_{us}\cdot\frac{a_y(s)}{\delta_f(s)}\right] \\ \frac{\gamma(s)}{\delta_f(s)} &= \frac{1}{\eta}\cdot\frac{1}{\tau s+1}\cdot\frac{V_x}{L}\cdot\left(1 - k_\delta - K_{us}\cdot\frac{a_y(s)}{\delta_f(s)}\right) \\ &\quad - \frac{1}{\tau s+1}\cdot\left(\frac{1}{\eta} - 1\right)\cdot\frac{\gamma(s)}{\delta_f(s)} \end{aligned} \quad \text{(A.31)}$$

Transpose the yaw rate term to the left, and replace k_δ using (8). And then, equation (A.32) is expressed as follows:

$$\frac{\gamma(s)}{\delta_f(s)} = \frac{1}{\eta\tau s+1}\cdot\frac{V_x}{L}\cdot\left(1 - \frac{\delta_{r,ss}(s)}{\delta_f(s)} - K_{us}\cdot\frac{a_y(s)}{\delta_f(s)}\right) \quad \text{(A.32)}$$

APPENDIX B
DERIVATION PROCESS OF (19)

By substituting equation (18) into equation (13), vehicle lateral response with proposed algorithm is derived as

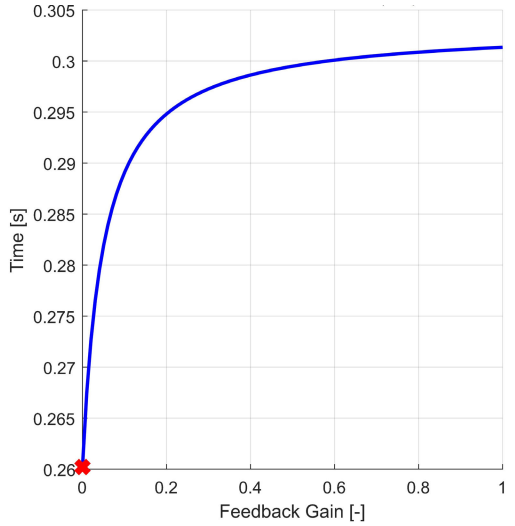

(a) Peak response time

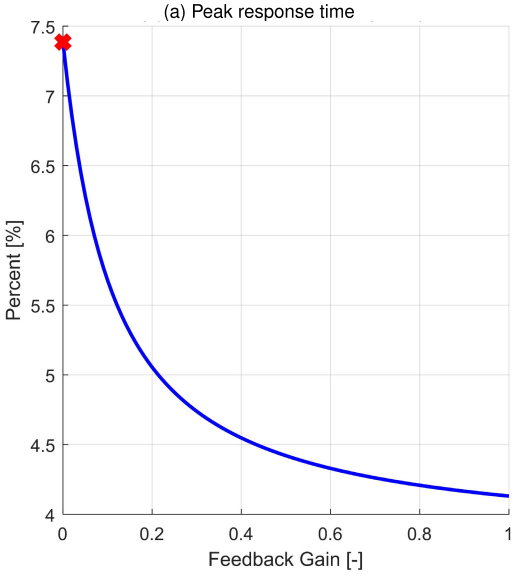

(b) Overshoot of yaw rate

FIGURE 20. Illustration of peak response time and overshoot in step steer scenario at 30 kph, 45 deg (300 deg/s), dry asphalt, with vehicle parameters in Table 1.

follows:

$$\begin{aligned}
&\frac{\gamma(s)}{\delta_f(s)} \\
&= \frac{1}{\tau s+1}\cdot\frac{V_x}{L} \\
&\quad\times\left[1-k_\delta-\left(\frac{1}{\eta}-1\right)\cdot(k_\delta-1)-\left(\frac{1}{\eta}-1\right)\cdot K_{us}\cdot\frac{a_y(s)}{\delta_f(s)}\right. \\
&\quad-\left(\frac{1}{\eta}-1\right)\cdot\frac{L}{V_x}\cdot\frac{\gamma(s)}{\delta_f(s)}+K_{fb}\cdot\left(\frac{a_y(s)}{\delta_f(s)}-V_x\frac{\gamma(s)}{\delta_f(s)}\right) \\
&\quad\left.-K_{us}\cdot\frac{a_y(s)}{\delta_f(s)}\right] \qquad \text{(B.33)} \\
&(\tau s+1)\,\frac{\gamma(s)}{\delta_f(s)} \\
&=\frac{1}{\eta}\cdot\frac{V_x}{L}\cdot\left[1-k_\delta-\left(K_{us}-\eta K_{fb}\right)\cdot\frac{a_y(s)}{\delta_f(s)}\right]
\end{aligned}$$

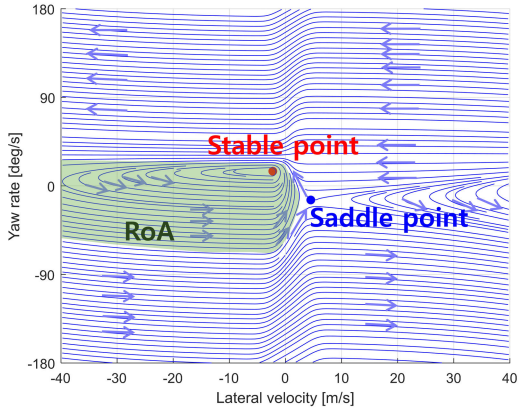

(a) Base (passive vehicle)

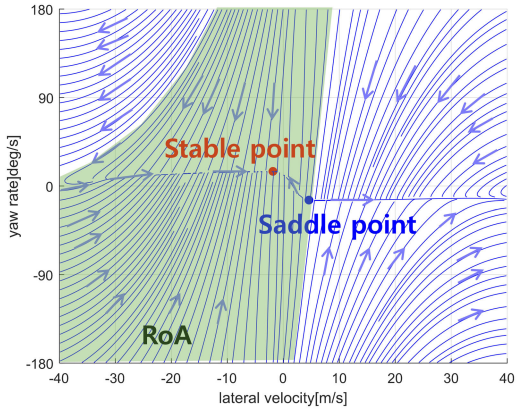

(b) Proposed RWS vehicle

FIGURE 21. Vy - Yaw rate phase plane.

$$-\frac{1}{\eta}\cdot\left(1-\eta+\eta K_{fb}\frac{V_x^2}{L}\right)\cdot\frac{L}{V_x}\cdot\frac{\gamma(s)}{\delta_f(s)} \qquad \text{(B.34)}$$

By summarizing equation (B.34), the yaw rate response to the driver's steering input is expressed as follows:

$$\begin{aligned}
\frac{\gamma(s)}{\delta_f(s)} &= \frac{1}{\eta_f\tau s+1}\cdot\frac{\eta_f}{\eta} \\
&\quad\times\frac{V_x}{L}\left[1-k_\delta-\left(K_{us}-\eta K_{fb}\right)\cdot\frac{a_y(s)}{\delta_f(s)}\right] \\
\eta_f &= \frac{\eta}{1+\frac{\eta K_{fb}V_x^2}{L}} \qquad \text{(B.35)}
\end{aligned}$$

APPENDIX C
TRANSIENT RESPONSES OF VEHICLE YAW RATE AT 30kph

The peak time and the peak yaw rate at 30 kph of vehicle speed were calculated from (25). The peak response time and overshoot are shown in Figure 20.

APPENDIX D
THE STABILITY ISSUE OF THE PROPOSED CONTROL ALGORITHM

The stability of the proposed control algorithm has been described in this section. The proposed algorithm is based

on the parameterization afforded by offline numerical optimization. However, there is no guarantee from the stability point of view. Thus, the proposed algorithm has been verified whether the controller can extend the region of attraction on the phase plane.

The results of the phase portrait are analyzed under assumptions of constant steering wheel angle 45deg and vehicle speed 110kph. The region of attraction (RoA) converging to the stable node is represented as green area in Figure 21. It can be shown that the proposed algorithm expands the RoA compared to the uncontrolled vehicle.

REFERENCES

[1] Y. Furukawa, N. Yuhara, S. Sano, H. Takeda, and Y. Matsushita, "A review of four-wheel steering studies from the viewpoint of vehicle dynamics and control," *Vehicle Syst. Dyn.*, vol. 18, nos. 1–3, pp. 151–186, Jan. 1989.
[2] M. Nagai, Y. Hirano, and S. Yamanaka, "Integrated control of active rear wheel steering and direct yaw moment control," *Vehicle Syst. Dyn.*, vol. 27, nos. 5–6, pp. 357–370, Jun. 1997.
[3] S.-H. Lee, U.-K. Lee, S.-K. Ha, and C.-S. Han, "Four-wheel independent steering (4WIS) system for vehicle handling improvement by active rear toe Control," *JSME Int. J. Ser. C, Mech. Syst., Mach. Elements Manuf.*, vol. 42, no. 4, pp. 947–956, 1999.
[4] T. Eguchi, Y. Sakita, K. Kawagoe, S. Kaneko, K. Mori, and T. Matsumoto, "Development of 'super Hicas', a new rear wheel steering system with phasereversal control," *SAE Trans.*, vol. 98, no. 891978, pp. 1495–1504, 1989.
[5] H. M. Lv and N. C. P. Li, "Multi-objective H∞ optimal control for four-wheel steering vehicle based on yaw rate tracking," *Proc. Inst. Mech. Eng., Part D, J. Automobile Eng.*, vol. 218, no. 10, pp. 1117–1123, 2004.
[6] S. Wagner, J. M. Schilling, J. L. Braun, and G. Prokop, "Design and assessment of optimal feedforward control for active steering configurations in passenger vehicles," *Vehicle Syst. Dyn.*, vol. 55, no. 8, pp. 1123–1142, Aug. 2017.
[7] M. Abe, "Vehicle dynamics and control for improving handling and active safety: From four-wheel steering to direct yaw moment control," *Proc. Inst. Mech. Eng., K, J. Multi-Body Dyn.*, vol. 213, no. 2, pp. 87–101, Dec. 1999.
[8] P. Zarco and A. G. Exposito, "Power system parameter estimation: A survey," *IEEE Trans. Power Syst.*, vol. 15, no. 1, pp. 216–222, Feb. 2000.
[9] J. Rissanen, "Performance deterioration of optimum systems," *IEEE Trans. Autom. Control*, vol. 11, no. 3, pp. 530–532, Jul. 1966.
[10] S. O. T. Ogaji, S. Sampath, R. Singh, and S. D. Probert, "Parameter selection for diagnosing a gas-turbine's performance-deterioration," *Appl. Energy*, vol. 73, no. 1, pp. 25–46, Sep. 2002.
[11] H. E. B. Russell and J. C. Gerdes, "Design of variable vehicle handling characteristics using four-wheel steer-by-wire," *IEEE Trans. Control Syst. Technol.*, vol. 24, no. 5, pp. 1529–1540, Sep. 2016.
[12] M. Akar, "Yaw rate and sideslip tracking for 4-Wheel steering cars using sliding mode control," in *Proc. IEEE Conf. Comput. Aided Control Syst. Design, IEEE Int. Conf. Control Appl., IEEE Int. Symp. Intell. Control*, Oct. 2006, pp. 1300–1305.
[13] L. Bredthauer and D. Lynch, "Use of active rear steering to achieve desired vehicle transient lateral dynamics," SAE Tech. Paper 2018-01-0565, 2018, doi: 10.4271/2018-01-0565.
[14] Y. H. Cho and J. Kim, "Design of optimal four-wheel steering system," *Vehicle Syst. Dyn.*, vol. 24, no. 9, pp. 661–682, Oct. 1995.
[15] N. Irie and J. Kuroki, "4WS technology and the prospects for improvement of vehicle dynamics," in *Proc. Vehicle Electron. Int. Congr. Transp. Electron.*, Oct. 1990, pp. 428–437.
[16] K. Uno, *Vehicle Dynamic Performance and Chassis Mechanism*. Japan: Grand Prix Book Publishing 1994, pp. 265–275.
[17] R. Rajamani, *Vehicle Dynamics and Control*. New York, NY, USA: Springer, 2011.
[18] M. Tanelli, S. Savaresi, and C. Cantoni, "Longitudinal vehicle speed estimation for traction and braking control systems," in *Proc. IEEE Conf. Comput. Aided Control Syst. Design, IEEE Int. Conf. Control Appl., IEEE Int. Symp. Intell. Control*, Oct. 2006, pp. 2790–2795.
[19] K. Ogata and Y. Yang, *Modern Control Engineering*, vol. 5. Upper Saddle River, NJ, USA: Prentice-Hall, 2010.
[20] C. L. Phillips and R. D. Habor, *Feedback Control Systems*. New York, NY, USA: Simon & Schuster, Inc., 1995.
[21] C. I. Byrnes, D. S. Gilliam, and J. He, "Root-locus and boundary feedback design for a class of distributed parameter systems," *SIAM J. Control Optim.*, vol. 32, no. 5, pp. 1364–1427, Sep. 1994.
[22] J. L. Moiola, M. C. Colantonio, and P. D. Doñate, "Analysis of static and dynamic bifurcations from a feedback systems perspective," *Dyn. Stability Syst.*, vol. 12, no. 4, pp. 293–317, Jan. 1997.
[23] G. Gu, X. Chen, A. G. Sparks, and S. S. Banda, "Bifurcation stabilization with local output feedback," *SIAM J. Control Optim.*, vol. 37, no. 3, pp. 934–956, Jan. 1999.
[24] J. Schuller, I. Haque, and M. Eckel, "An approach for optimisation of vehicle handling behaviour in simulation," *Vehicle Syst. Dyn.*, vol. 37, no. 1, pp. 24–37, Jan. 2002.
[25] S. R. Fetrati, C. Kandler C. Kärcher, and D. Schramm, "Inversion based feedforward design to improve the lateral dynamics of high performance sports cars," in *Proc. 13th Int. Symp. Adv. Vehicle Control*, 2016, pp. 625–629.
[26] A. Y. Lee, "Performance of four-wheel-steering vehicles in lane change maneuvers," SAE Tech. Paper 950316, 1995.
[27] S. Sivaramakrishnan and S. Taheri, "Using objective vehicle-handling metrics for tire performance evaluation and selection," *SAE Int. J. Passenger Cars-Mech. Syst.*, vol. 6, no. 2, pp. 732–740, 2013.

KWANWOO PARK received the B.S. and M.S. degrees in mechanical engineering from Seoul National University, South Korea, in 2015 and 2017, respectively, where he is currently pursuing the Ph.D. degree in mechanical engineering. His research interests include vehicle stability control, vehicle dynamics, vehicle handling performance, and rear-wheel steering vehicle.

EUNHYEK JOA received the B.S. and M.S. degrees in mechanical engineering from Seoul National University, South Korea, in 2014 and 2016, respectively. He is currently pursuing the Ph.D. degree in mechanical engineering with the University of California at Berkeley. His research interests include vehicle stability control, vehicle dynamics, and motion predictive control.

KYONGSU YI (Member, IEEE) received the B.S. and M.S. degrees in mechanical engineering from Seoul National University, South Korea, in 1985 and 1987, respectively, and the Ph.D. degree in mechanical engineering from the University of California at Berkeley, in 1992.

He is currently a Professor with the School of Mechanical Engineering, Seoul National University. His research interests include control systems, driver assistant systems, and active safety systems of ground vehicles. He also serves as a member of the Editorial Board of the KSME, IJAT, and ICROS journals.

YOUNGSIK YOON received the B.S. degree in mechanical engineering from Sungkyunkwan University, South Korea, in 2009, and the M.S degree from the Korea Advanced Institute of Science and Technology (KAIST), South Korea, in 2011.

He is currently a Senior Research Engineer with the Chassis Control Logic Development Team, Hyundai Motor Company R&D Center, South Korea. He is working on integrated chassis control in conjunction with rear-wheel steering systems.